

**“Supporting Information”**

**Design and synthesis of hydrophobic mixed organogel with complementary hydrogen-bond donor-acceptor sites: removal of heavy metal ions  $\text{Hg}^{+2}$ ,  $\text{Cd}^{+2}$  and  $\text{Pb}^{+2}$  from aqueous solution**

Reena Kyarikwal,<sup>a</sup> Ritika Munjal,<sup>a</sup> Probal Nag,<sup>b</sup> Sivarajana Reddy Vennapusa<sup>b</sup> and Suman Mukhopadhyay<sup>a\*</sup>

<sup>a</sup>Department of Chemistry, School of basic science, Indian Institute of Technology Indore, Khandwa Road, Simrol, Indore, 453552, India

<sup>b</sup>School of Chemistry, Indian Institute of Science Education and Research Thiruvananthapuram, Thiruvananthapuram 695551, India

\*Email: [suman@iiti.ac.in](mailto:suman@iiti.ac.in)

**Table of Contents**

**Fig. S1:** ESI-MS data of gelator component **GE**.

**Fig. S2:**  $^1\text{H}$  NMR data of gelator component **GE**.

**Fig. S3:**  $^{13}\text{C}$  NMR data of gelator component **GE**.

**Fig. S4:** FTIR data of gelator enhancer molecule **GE**.

**Fig. S5:** Angular sweep experiment of organogel **G8GE** with (a) 0.01: 0.01 mmol (b) 0.02: 0.02 mmol in 1:1 ratio of 2 mL DMSO:  $\text{H}_2\text{O}$  mixture.

**Fig. S6:** Angular sweep experiment of organogel **G8GE** with (a) 0.03: 0.03 mmol (b) 0.04: 0.04 mmol in 1:1 ratio of 2 mL DMSO:  $\text{H}_2\text{O}$  mixture.

**Fig. S7:** Angular sweep experiment of organogel **G8GE** with (a) 0.07: 0.07 mmol (b) 0.1: 0.1 mmol in 1:1 ratio of 2 mL DMSO:  $\text{H}_2\text{O}$  mixture.

**Table S1:** Concentration dependent rheological study of organogel **G8GE**.

**Fig. S8:** UV-Vis spectrum of (a) **GE** and (c) **G8GE**.

**Fig. S9:** Fluorescence spectrum of (a) **G8**, **GE**, **G8GE** (b) 1 mM solution of **G8**, **GE** and **G8GE** under UV chamber.

**Fig. S10:** (a) Fluorescence study of **G8GE** gelator component with different polar protic and polar aprotic solvents (b) 0.3 mM solution of **G8GE** component in different solvents under UV chamber.

**Fig. S11:** Fluorescence study of **G8GE** organogel and metallogels formed by (a) mixing method and (b) adsorption method.

**Fig. S12:** Fluorescence study of (a) 1 mM solution of **G8GE** (in DMSO) and  $\text{HgCl}_2$  (in  $\text{H}_2\text{O}$ ) and (b) 1 mM solution of **G8GE** (in DMSO:  $\text{H}_2\text{O}$ ) and  $\text{HgCl}_2$  (in DMSO:  $\text{H}_2\text{O}$ ).

**Fig. S13:** FE-SEM images of (a) **M1G8GECl<sub>2</sub>Ads** (b) **M1G8GE(OAc)<sub>2</sub>Ads** (c) **M1G8GESO<sub>4</sub>Ads** (d) **M2G8GECl<sub>2</sub>Ads** (e) **M2G8GE(OAc)<sub>2</sub>Ads** (f) **M2G8GESO<sub>4</sub>Ads** (g) **M3G8GECl<sub>2</sub>Ads** and (h) **M3G8GE(OAc)<sub>2</sub>Ads** formed by adsorption method.

**Fig. S14:** EDX and Mapping analysis of **M1G8GECl<sub>2</sub>** showing the presence of C, N, O, Hg and Cl inside gel matrix.

**Fig. S15:** EDX and Mapping analysis of **M1G8GE(OAc)<sub>2</sub>** showing the presence of C, N, O and Hg inside gel matrix.

**Fig. S16:** EDX and Mapping analysis of **M1G8GESO<sub>4</sub>** showing the presence of C, N, O, Hg and S inside gel matrix.

**Fig. S17:** EDX and Mapping analysis of **M2G8GECl<sub>2</sub>** showing the presence of C, N, O, Cd and Cl inside gel matrix.

**Fig. S18:** EDX and Mapping analysis of **M2G8GE(OAc)<sub>2</sub>** showing the presence of C, N, O and Cd inside gel matrix.

**Fig. S19:** EDX and Mapping analysis of **M2G8GESO<sub>4</sub>** showing the presence of C, N, O, Cd and S inside gel matrix.

**Fig. S20:** EDX and Mapping analysis of **M3G8GECl<sub>2</sub>** showing the presence of C, N, O, Pb and Cl inside gel matrix.

**Fig. S21:** EDX and Mapping analysis of **M3G8GE(OAc)<sub>2</sub>** showing the presence of C, N, O and Pb inside gel matrix.

**Fig. S22:** (a) Frequency sweep experiment of organogel **G8GE** at 1:1 molar ratio (0.03: 0.03 mmol) (b) Frequency sweep experiment of organogel **G8GE** at 3: 2 molar ratio (0.03: 0.02 mmol).

**Fig. S23:** (a) Angular sweep experiment of metallogel **M1G8GECl<sub>2</sub>** (b) Frequency sweep experiment of metallogel **M1G8GECl<sub>2</sub>**.

**Fig. S24:** (a) Angular sweep experiment of metallogel **M1G8GE(OAc)<sub>2</sub>** (b) Frequency sweep experiment of metallogel **M1G8GE(OAc)<sub>2</sub>**.

**Fig. S25:** (a) Angular sweep experiment of metallogel **M1G8GESO<sub>4</sub>** (b) Frequency sweep experiment of metallogel **M1G8GESO<sub>4</sub>**.

**Fig. S26:** (a) Angular sweep experiment of metallogel **M2G8GECl<sub>2</sub>** (b) Frequency sweep experiment of metallogel **M2G8GECl<sub>2</sub>**.

**Fig. S27:** (a) Angular sweep experiment of metallogel **M3G8GECl<sub>2</sub>** (b) Frequency sweep experiment of metallogel **M3G8GECl<sub>2</sub>**.

**Fig. S28:** (a) Angular sweep experiment of metallogel **M3G8GESO<sub>4</sub>** (b) Frequency sweep experiment of metallogel **M3G8GESO<sub>4</sub>**.

**Table S2:** Storage modulus and loss modulus of metallogels formed by mixing method.

**Fig. S29:** (a) Angular sweep experiment of metallogel **M1G8GECl<sub>2</sub>Ads** (b) Frequency sweep experiment of metallogel **M1G8GECl<sub>2</sub>Ads**.

**Fig. S30:** (a) Angular sweep experiment of metallogel **M1G8GE(OAc)<sub>2</sub>Ads** (b) Frequency sweep experiment of metallogel **M1G8GE(OAc)<sub>2</sub>Ads**.

**Fig. S31:** (a) Angular sweep experiment of metallogel **M1G8GESO<sub>4</sub>Ads** (b) Frequency sweep experiment of metallogel **M1G8GESO<sub>4</sub>Ads**.

**Fig. S32:** (a) Angular sweep experiment of metallogel **M2G8GECl<sub>2</sub>Ads** (b) Frequency sweep experiment of metallogel **M2G8GECl<sub>2</sub>Ads**.

**Fig. S33:** (a) Angular sweep experiment of metallogel **M2G8GE(OAc)<sub>2</sub>Ads** (b) Frequency sweep experiment of metallogel **M2G8GE(OAc)<sub>2</sub>Ads**.

**Fig. S34:** (a) Angular sweep experiment of metallogel **M2G8GESO<sub>4</sub>Ads** (b) Frequency sweep experiment of metallogel **M2G8GESO<sub>4</sub>Ads**.

**Fig. S35:** (a) Angular sweep experiment of metallogel **M3G8GECl<sub>2</sub>Ads** (b) Frequency sweep experiment of metallogel **M3G8GECl<sub>2</sub>Ads**.

**Fig. S36:** (a) Angular sweep experiment of metallogel **M3G8GE(OAc)<sub>2</sub>Ads** (b) Frequency sweep experiment of metallogel **M3G8GE(OAc)<sub>2</sub>Ads**.

**Table S3:** Storage modulus and loss modulus of metallogels formed by adsorption method.

**Fig. S37:** DFT structure showing (a, b) Planarity of **G8** (c, d) Tilted structure of **GE** and (e, f) Less tilted structure of **G8GE** as compared to **GE** after interaction with **G8**.

**Fig. S38:** HOMO-LUMO energy orbitals of (a) **G8** and (b) **GE**.

**Fig. S39:** FTIR data analysis of (a) **M1G8GECl<sub>2</sub>** (b) **M1G8GE(OAc)<sub>2</sub>** (c) **M1G8GESO<sub>4</sub>** (d) **M2G8GECl<sub>2</sub>** (e) precipitate of **M2G8GE(OAc)<sub>2</sub>** (f) precipitate of **M2G8GESO<sub>4</sub>** (g) **M3G8GECl<sub>2</sub>** (h) **M3G8GE(OAc)<sub>2</sub>**.

**Fig. S40:** PXRD data of metallogels (a) **M1G8GECl<sub>2</sub>** (b) **M1G8GE(OAc)<sub>2</sub>** (c) **M1G8GESO<sub>4</sub>** (d) **M2G8GECl<sub>2</sub>** (e) precipitate of **M2G8GE(OAc)<sub>2</sub>** (f) precipitate of **M2G8GESO<sub>4</sub>** (g) **M3G8GECl<sub>2</sub>** (h) **M3G8GE(OAc)<sub>2</sub>**.

**Fig. S41:** PXRD data of metallogels (a) **M1G8GECl<sub>2</sub>Ads** (b) **M1G8GE(OAc)<sub>2</sub> Ads** (c) **M2G8GECl<sub>2</sub> Ads** (d) **M2G8GE(OAc)<sub>2</sub> Ads** (e) **M2G8GESO<sub>4</sub> Ads** (f) **M3G8GECl<sub>2</sub> Ads**.

**Table S4:** Optimization of heavy metal removal reaction by xerogel of organogel **G8GE**, analysed by ICP-AES.

**Table S5:** ICP-AES analysis of study of adsorption property of organogel **G8GE**.

**Table S6:** Adsorption capacity of various gel-based adsorbent.

**Fig. S42:** BET analysis data of (a) Xerogel **G8GE** before Hg(OAc)<sub>2</sub> adsorption (b) After Hg(OAc)<sub>2</sub> adsorption and (c) after Hg(OAc)<sub>2</sub> removal from xerogel **G8GE** or recovery of xerogel **G8GE**.

**Fig. S43:** XPS analysis of xerogel **G8GE** showing (a) C1s spectrum (b) N1s spectrum and (c) O1s spectrum.

**Fig. S44:** XPS analysis of xerogel **mtG8GE** showing (a) C1s spectrum (b) N1s spectrum and (c) O1s spectrum.

**Fig. S45:** XPS analysis of xerogel **mrG8GE** showing (a) C1s spectrum (b) N1s spectrum and (c) O1s spectrum and (d) Hg 4f spectrum.

**Table S7:** XPS peaks position of various groups for **G8GE**, **mtG8GE** and recovered **mrG8GE**.

**Fig. S46:** FE-SEM images of (a) **M1G8GECl<sub>2</sub>** gel by mixing (b) **M1G8GECl<sub>2</sub>Ads** by adsorption (c) **M1G8GECl<sub>2</sub>Ads** when **G8GE** inserted inside the aqueous solution of HgCl<sub>2</sub>.

**Table S8:** Recyclability of xerogel **G8GE** for heavy metal separation.

**Table S9:** Water remediation at different pH by xerogel **G8GE**.

**Fig. S47:** Time oscillation sweep experiment of organogel **G8GE** at (a) 0.02: 0.02 mmol (b) 0.03: 0.03 mmol and (c) 0.04: 0.04 mmol.

**Fig. S48:** Time oscillation sweep experiment of metallogel **M3G8GECl<sub>2</sub>**.

**Fig. S49:** Time oscillation sweep experiment of metallogel **M2G8GECl<sub>2</sub>Ads**.

**Fig. S50:** Time oscillation sweep experiment of metallogel (a) **M2G8GE(OAc)<sub>2</sub>Ads** and (b) **M2G8GESO<sub>4</sub>Ads**.

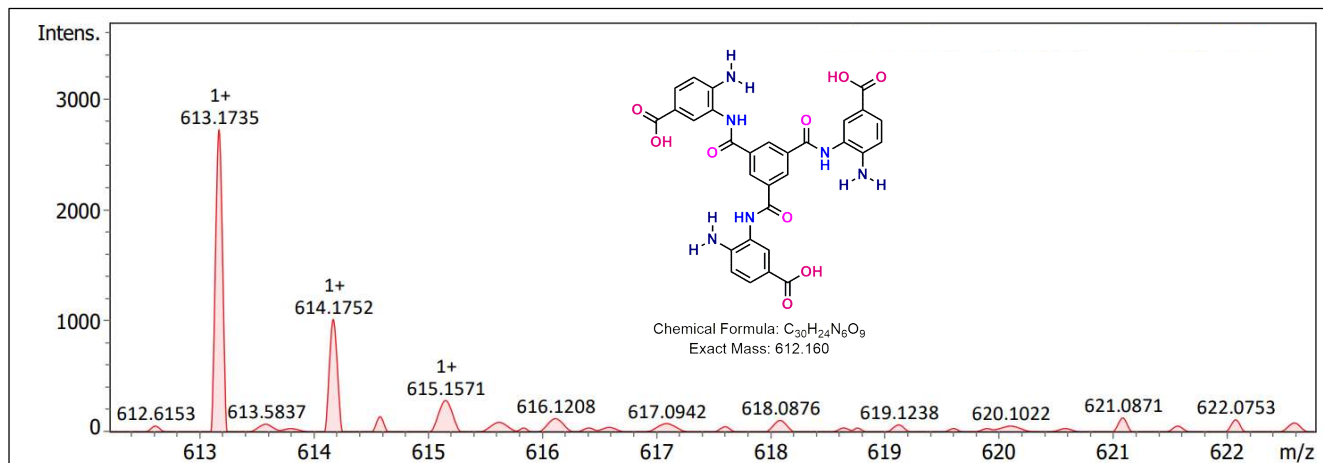
**Fig. S51:** Time oscillation sweep experiment of metallogel (a) **M3G8GECl<sub>2</sub>Ads** and (b) **M2G8GE(OAc)<sub>2</sub>Ads**.

**Table S10.** Intermolecular H-bond binding energies of individual sites along with the associated bond lengths of structure **G8GE**.

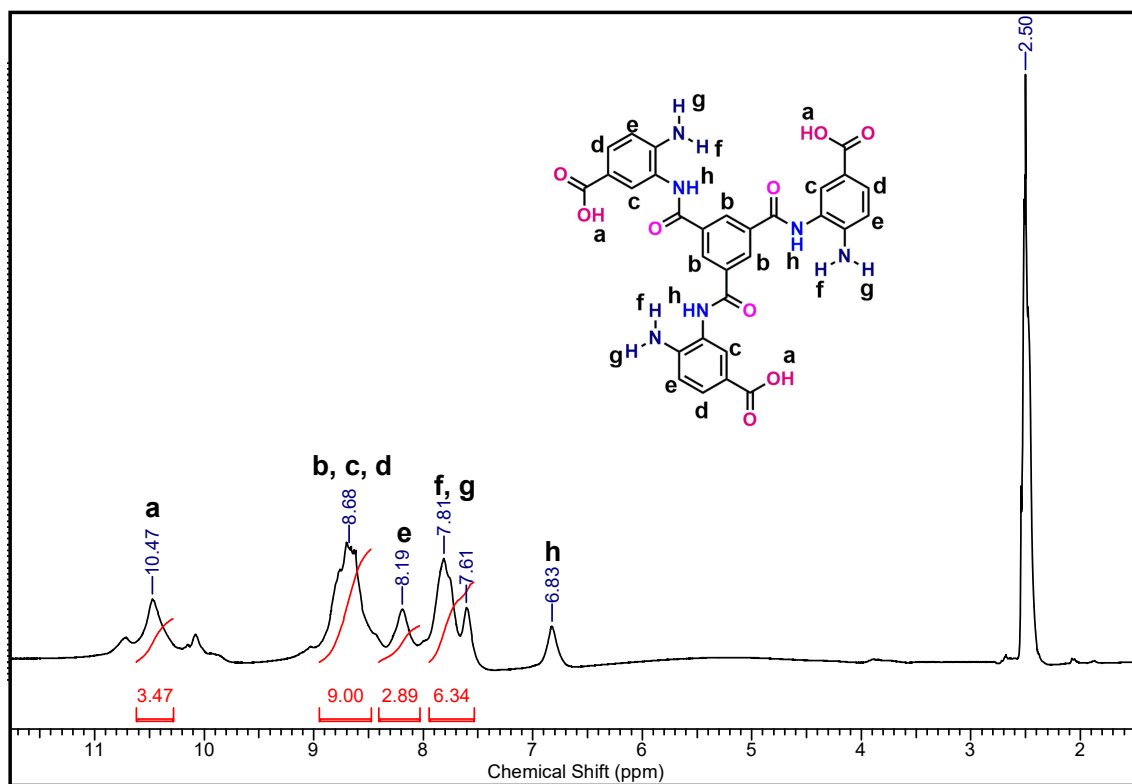
**Table S11.** Cartesian coordinates of **GE**.

**Table S12.** Cartesian coordinates of **G8**.

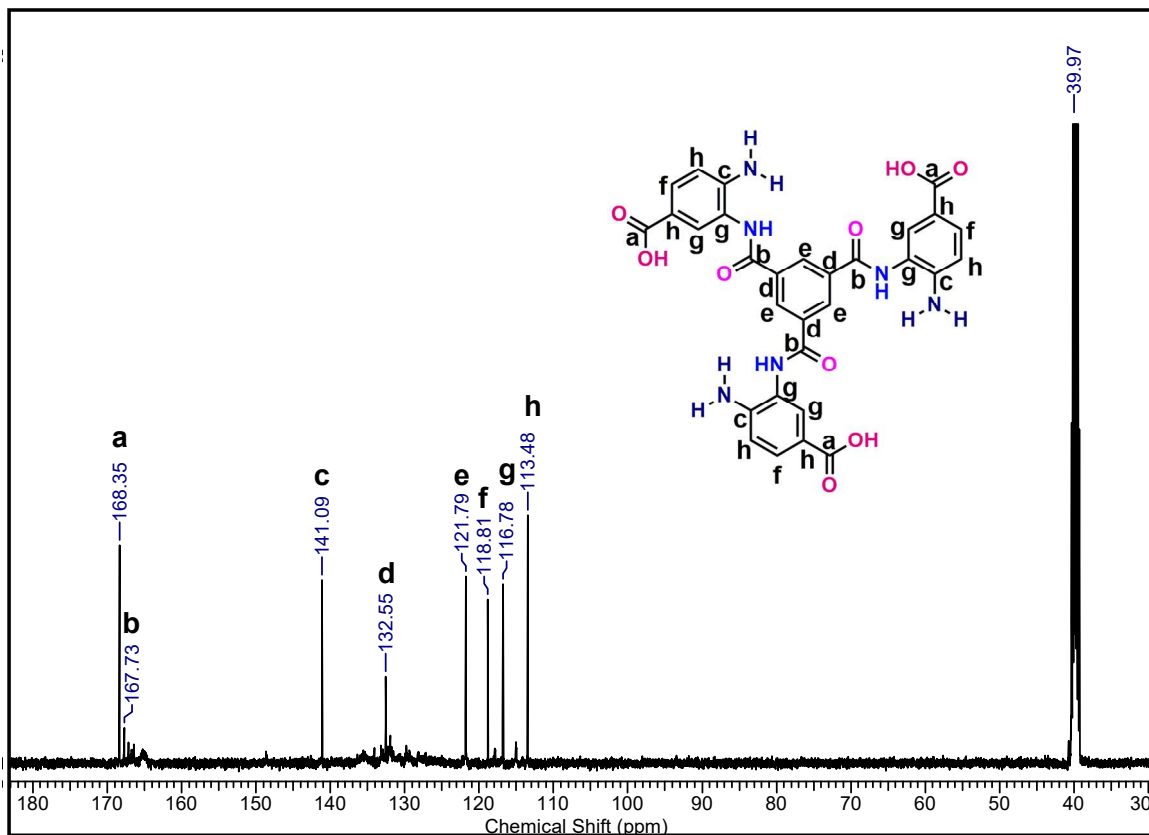
**Table S13.** Cartesian coordinates of **2GE-2G8 (G8GE)**.



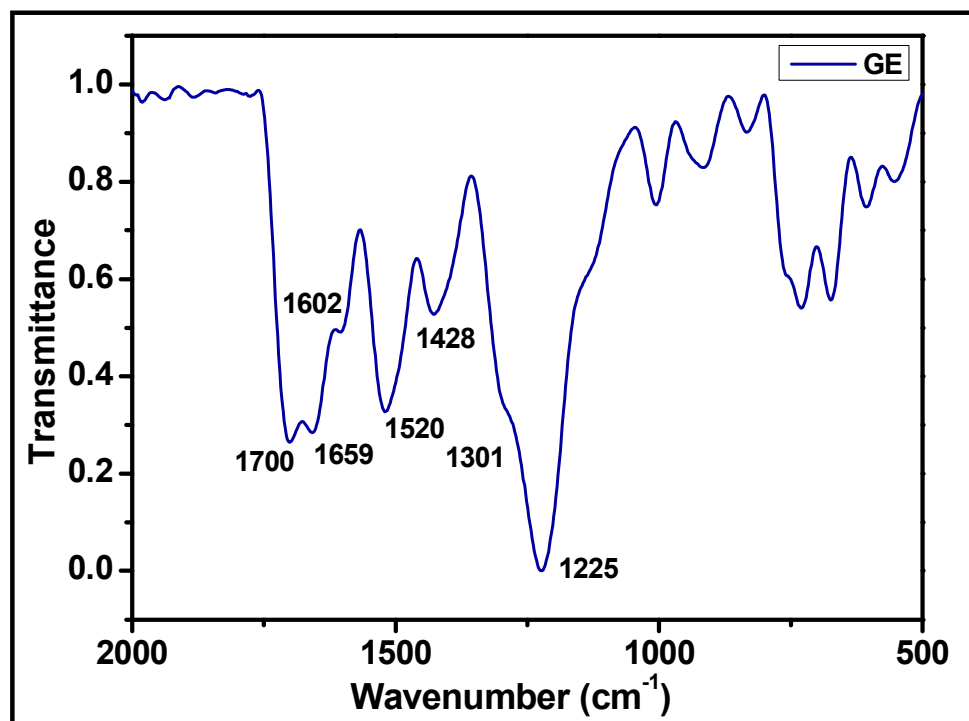
**Fig. S1:** ESI-MS data of gelator component **GE**.



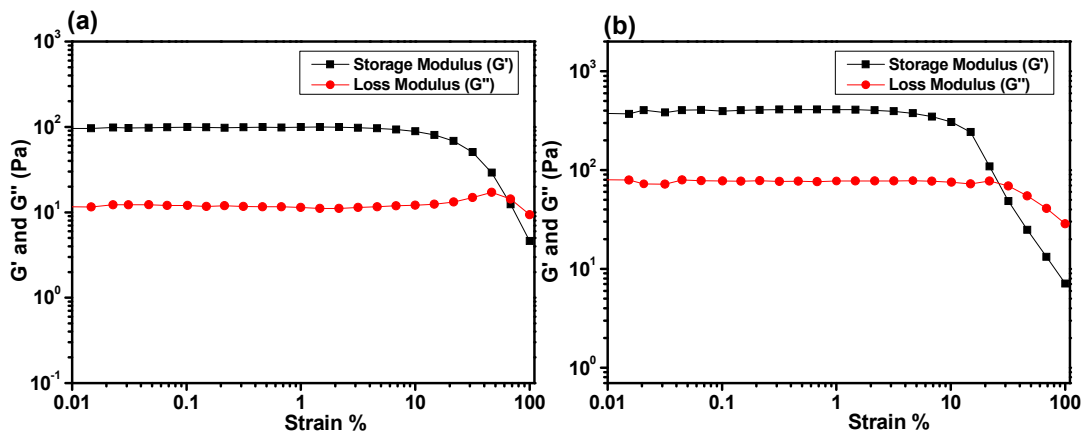
**Fig. S2:**  $^1\text{H}$  NMR data of gelator component **GE**.



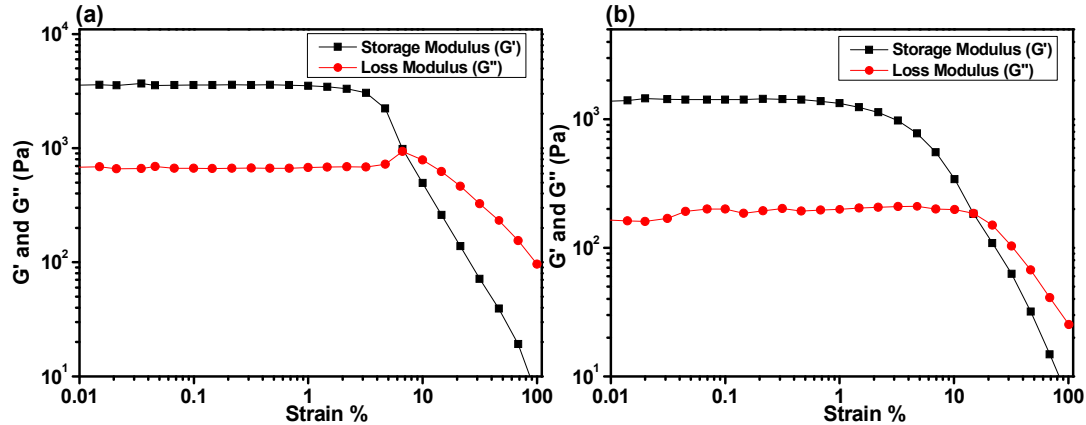
**Fig. S3:**  $^{13}\text{C}$  NMR data of gelator component **GE**.



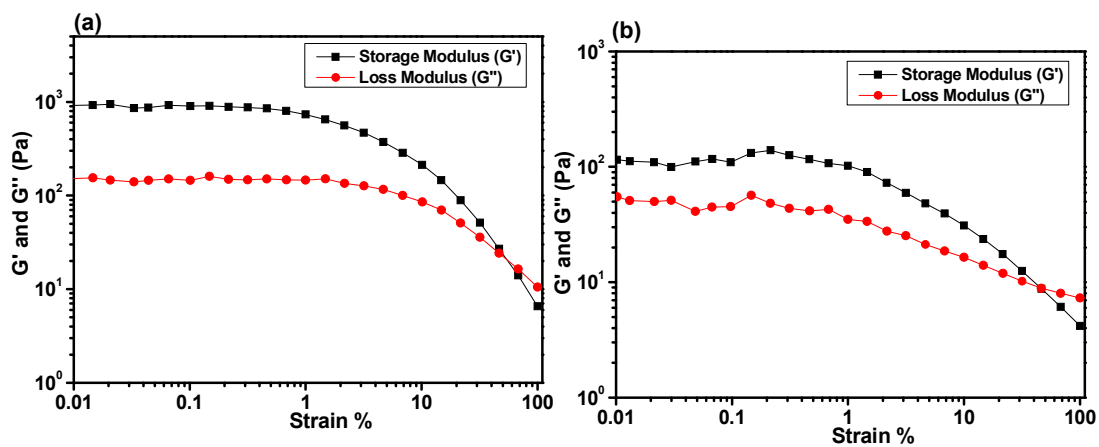
**Fig. S4:** FTIR data of gelator enhancer molecule **GE**.



**Fig. S5:** Angular sweep experiment of organogel **G8GE** with (a) 0.01: 0.01 mmol (b) 0.02: 0.02 mmol in 1:1 ratio of 2 mL DMSO:  $\text{H}_2\text{O}$  mixture.



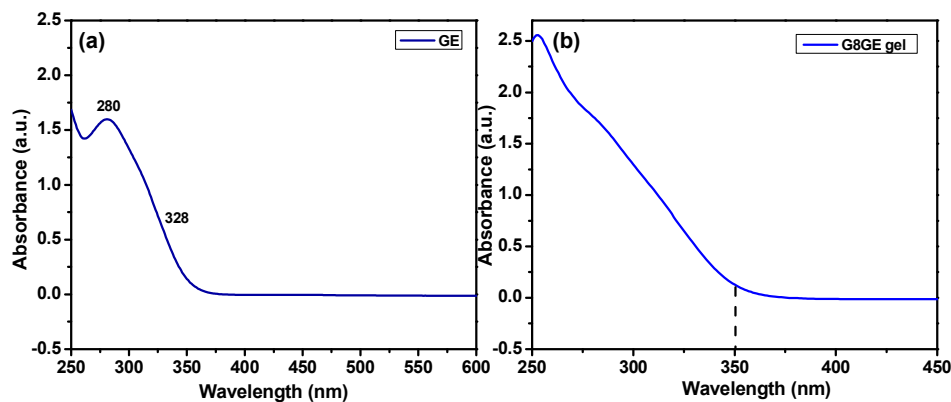
**Fig. S6:** Angular sweep experiment of organogel **G8GE** with (a) 0.03: 0.03 mmol (b) 0.04: 0.04 mmol in 1:1 ratio of 2 mL DMSO:  $\text{H}_2\text{O}$  mixture.



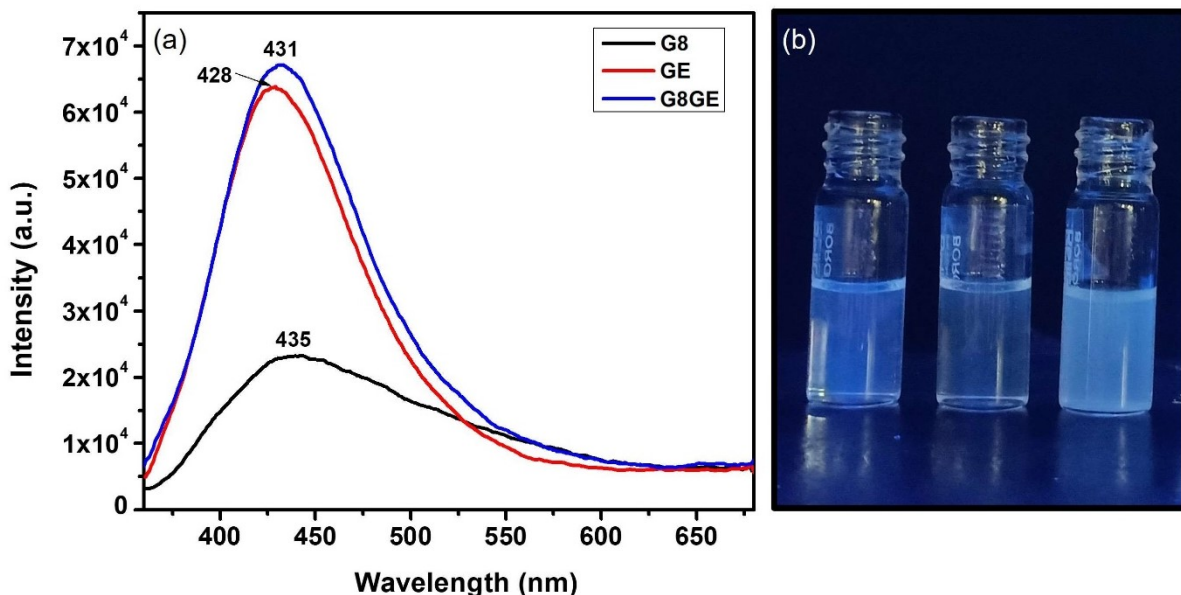
**Fig. S7:** Angular sweep experiment of organogel **G8GE** with (a) 0.07: 0.07 mmol (b) 0.1: 0.1 mmol in 1:1 ratio of 2 mL DMSO:  $\text{H}_2\text{O}$  mixture.

**Table S1:** Concentration dependent rheological study of organogel **G8GE**.

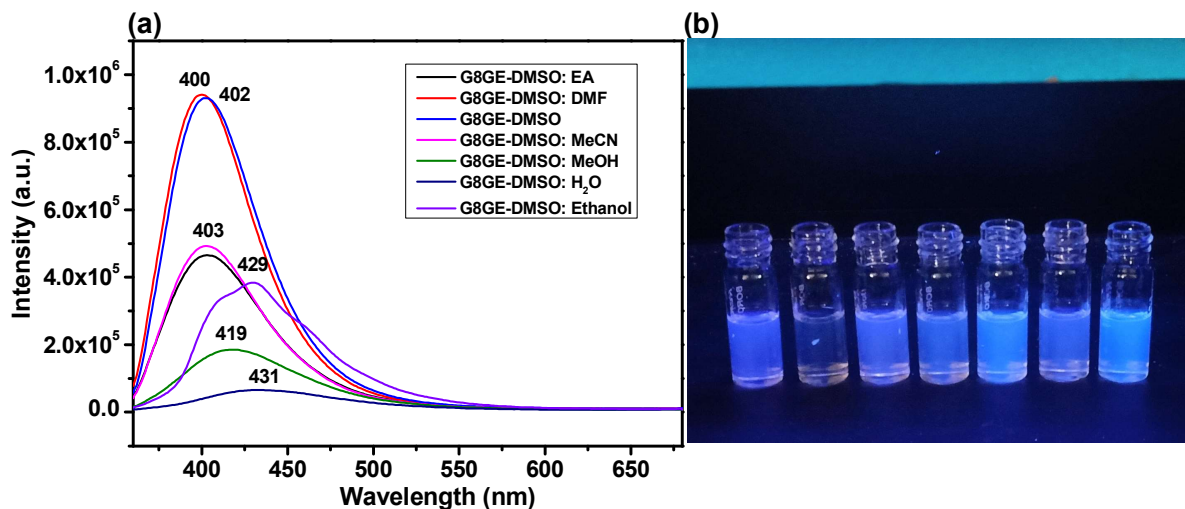
S. No.	mmol of G8	mmol of GE	Ratio of G8 and GE	Observation in 1 mL DMSO: 1 mL H <sub>2</sub> O	Value of G'	Value of crossover point	Non- deformation range
1	0.01	0.01	1:1	Gel	95 Pa	68 strain %	0.01- 4.85 strain %
2	0.02	0.02	1:1	Gel	392 Pa	26 strain %	0.01- 2.16 strain %
3	0.03	0.03	1:1	Strong Gel	3517 Pa	6 strain %	0.01- 1.01 strain %
4	0.04	0.04	1:1	Strong Gel	1456 Pa	14 strain %	0.01- 0.47 strain %
5	0.07	0.07	1:1	Gel	922 Pa	47 strain %	0.01- 0.22 strain %
6	0.1	0.1	1:1	Gel	144 Pa	46 strain %	0.01- 0.15 strain %
7	0.03	0.02	3:2	Strong Gel	1593 Pa	25 strain %	0.01- 2.16 strain %



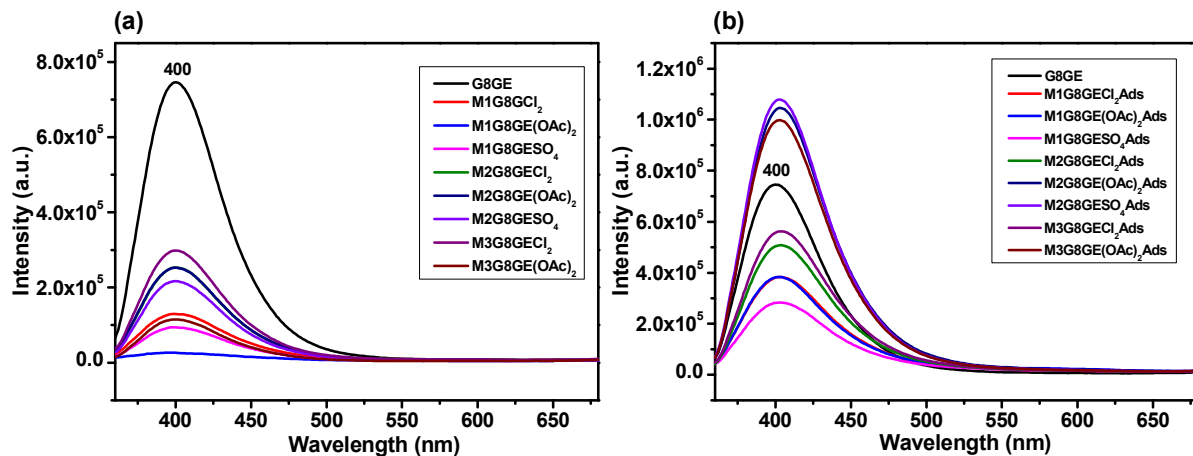
**Fig. S8:** UV-Vis spectrum of (a) **GE** and (c) **G8GE**.



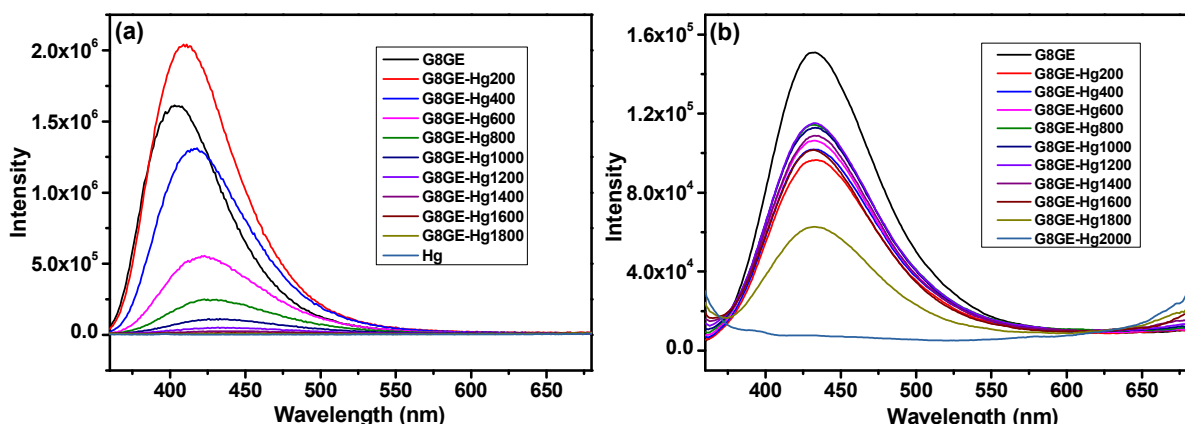
**Fig. S9:** Fluorescence spectrum of (a) **G8**, **GE**, **G8GE** (b) 1 mM solution of **G8**, **GE** and **G8GE** under UV chamber.



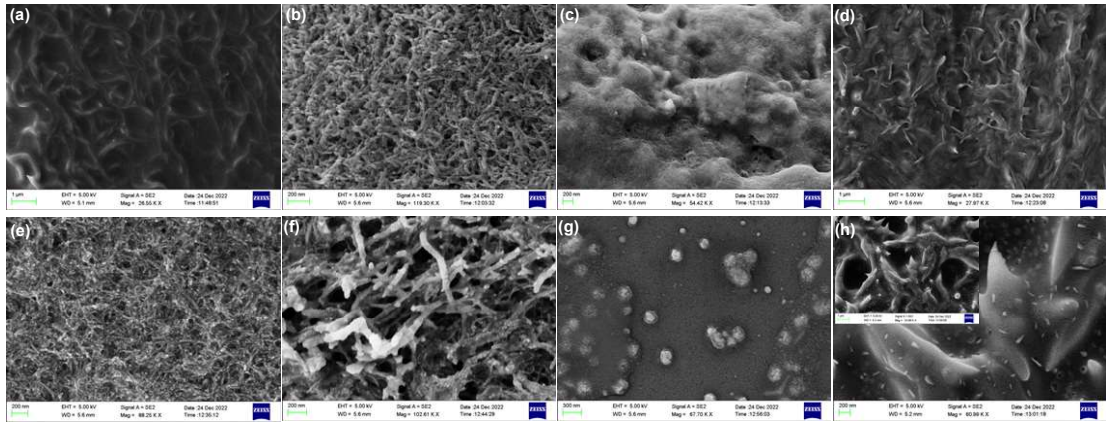
**Fig. S10:** (a) Fluorescence study of **G8GE** gelator component with different polar protic and polar aprotic solvents (b) 0.3 mM solution of **G8GE** component in different solvents under UV chamber.



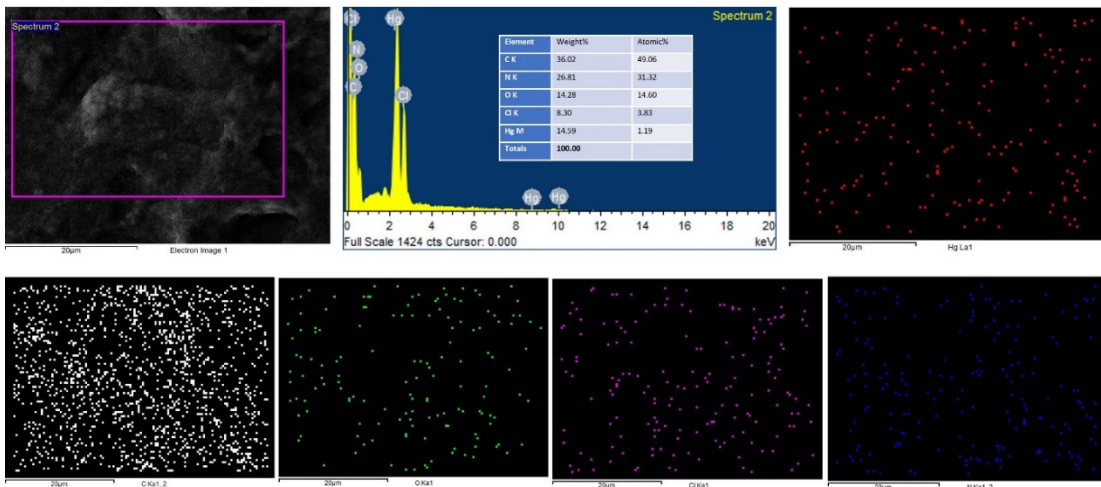
**Fig. S11:** Fluorescence study of **G8GE** organogel and metallogels formed by (a) mixing method and (b) adsorption method.



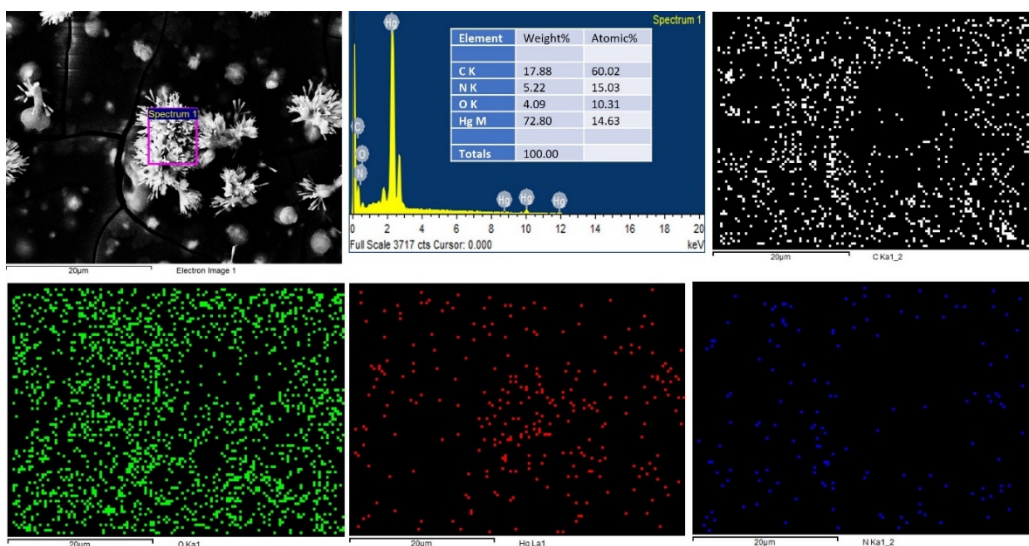
**Fig. S12:** Fluorescence study of (a) 1 mM solution of **G8GE** (in DMSO) and HgCl<sub>2</sub> (in H<sub>2</sub>O) and (b) 1 mM solution of **G8GE** (in DMSO: H<sub>2</sub>O) and HgCl<sub>2</sub> (in DMSO: H<sub>2</sub>O).



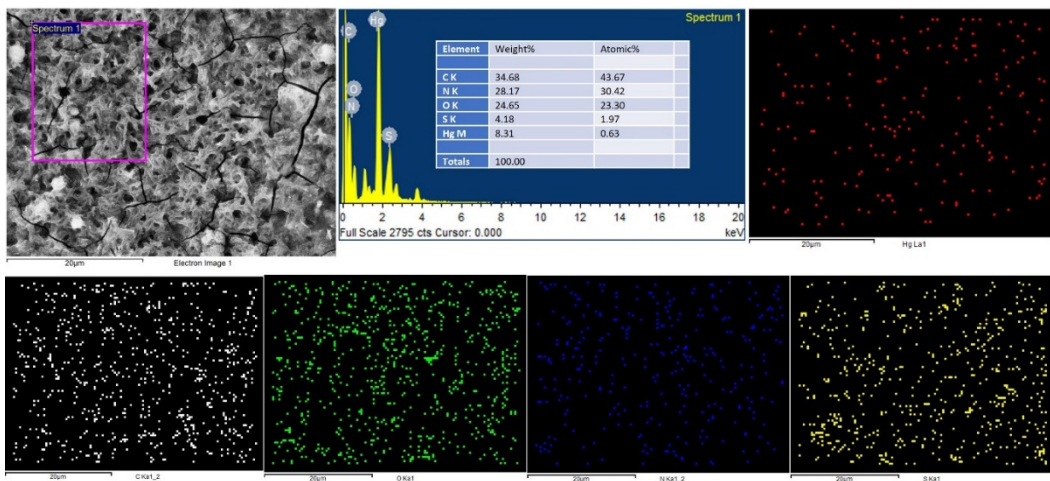
**Fig. S13:** FE-SEM images of (a) **M1G8GECl<sub>2</sub>Ads** (b) **M1G8GE(OAc)<sub>2</sub>Ads** (c) **M1G8GESO<sub>4</sub>Ads** (d) **M2G8GECl<sub>2</sub>Ads** (e) **M2G8GE(OAc)<sub>2</sub>Ads** (f) **M2G8GESO<sub>4</sub>Ads** (g) **M3G8GECl<sub>2</sub>Ads** and (h) **M3G8GE(OAc)<sub>2</sub>Ads** formed by adsorption method.



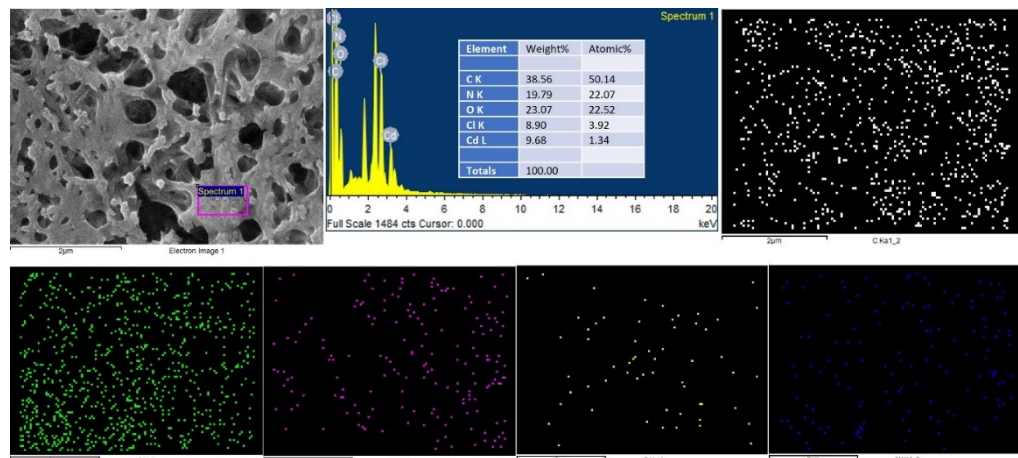
**Fig. S14:** EDX and Mapping analysis of **M1G8GECl<sub>2</sub>** showing the presence of C, N, O, Hg and Cl inside matrix.



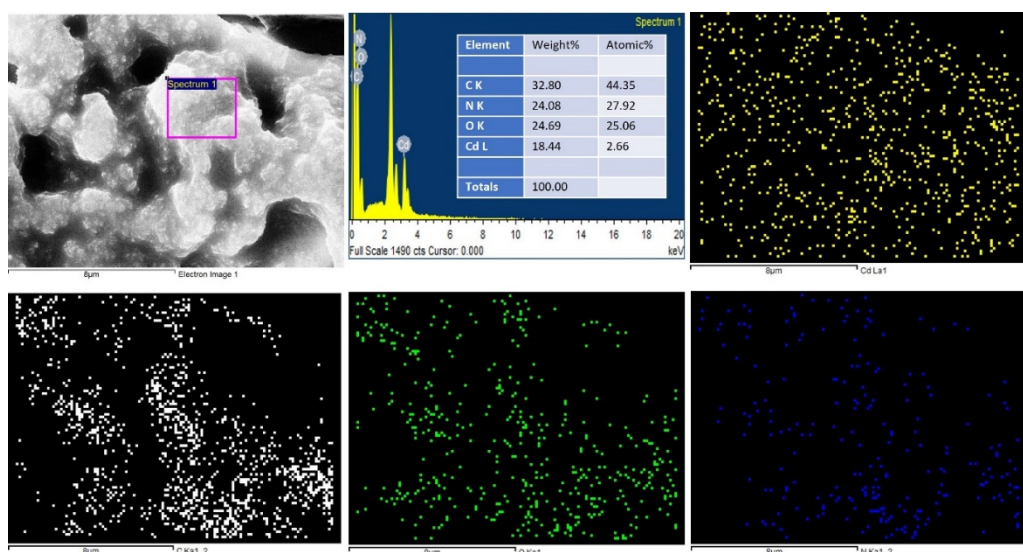
**Fig. S15:** EDX and Mapping analysis of **M1G8GE(OAc)<sub>2</sub>** showing the presence of C, N, O and Hg inside gel matrix.



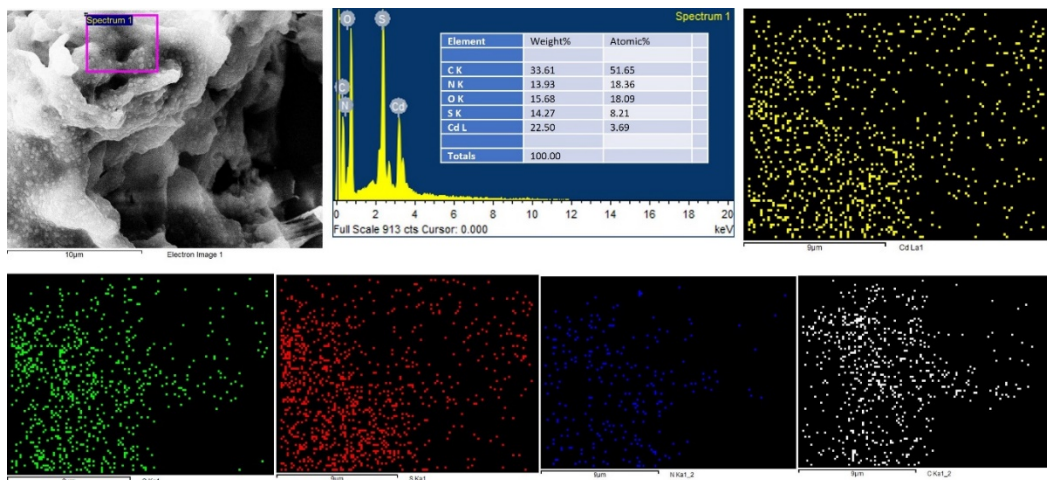
**Fig. S16:** EDX and Mapping analysis of **M1G8GESO<sub>4</sub>** showing the presence of C, N, O, Hg and S inside gel matrix.



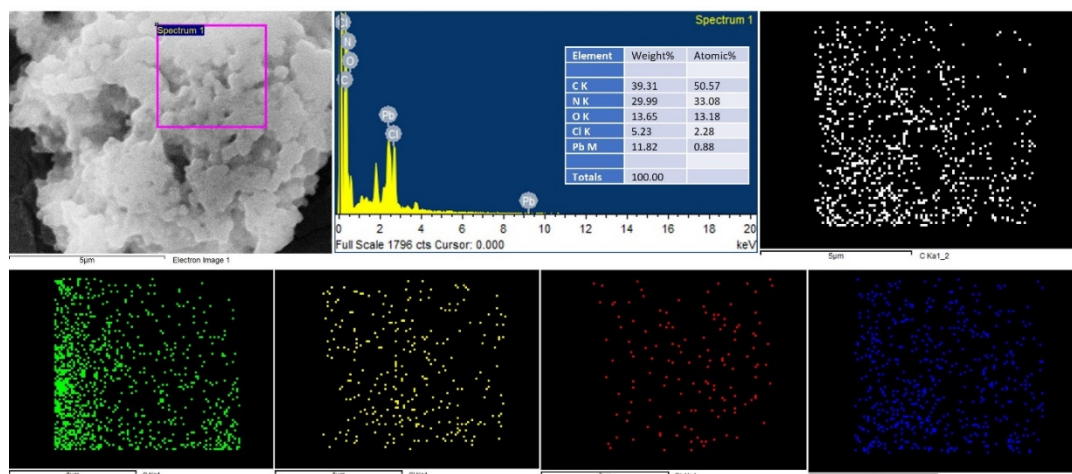
**Fig. S17:** EDX and Mapping analysis of **M2G8GECI<sub>2</sub>** showing the presence of C, N, O, Cd and Cl inside gel matrix.



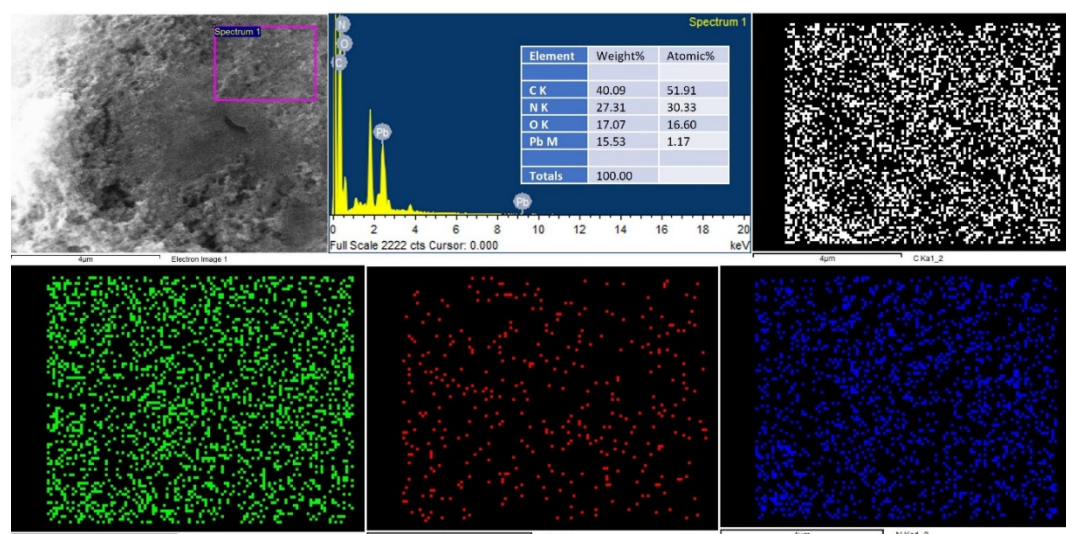
**Fig. S18:** EDX and Mapping analysis of **M2G8GE(OAc)<sub>2</sub>** showing the presence of C, N, O and Cd inside gel matrix.



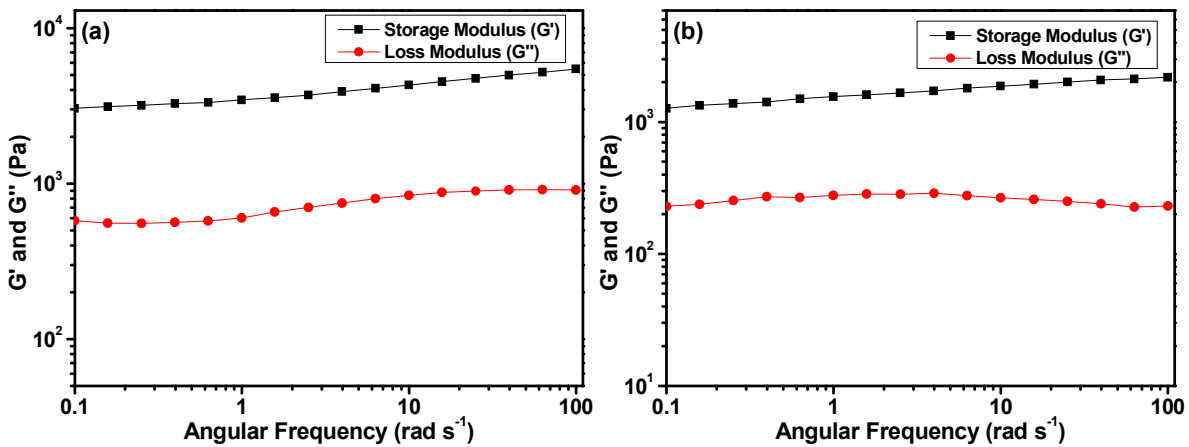
**Fig. S19:** EDX and Mapping analysis of **M<sub>2</sub>G<sub>8</sub>GESO<sub>4</sub>** showing the presence of C, N, O, Cd and S inside gel matrix.



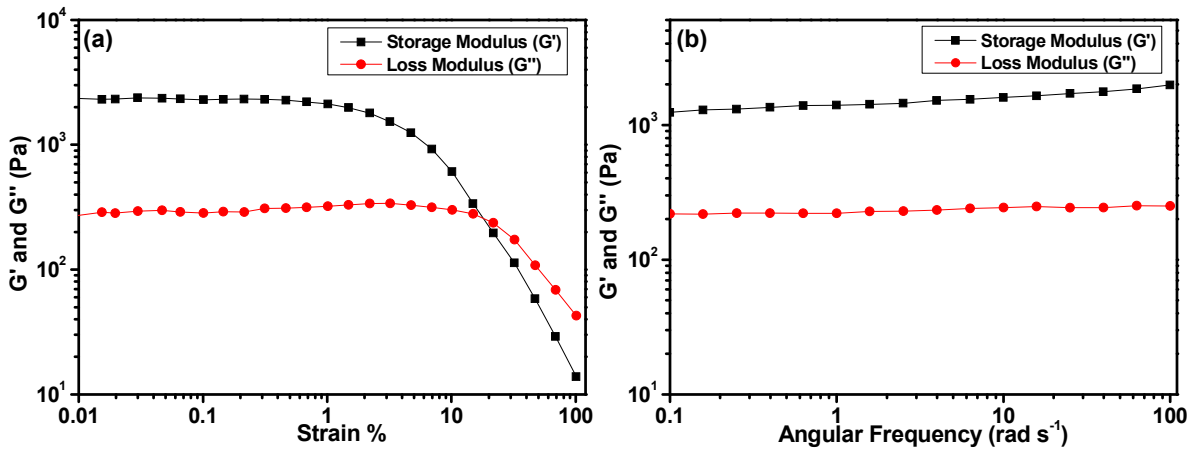
**Fig. S20:** EDX and Mapping analysis of **M<sub>3</sub>G<sub>8</sub>GECI<sub>2</sub>** showing the presence of C, N, O, Pb and Cl inside gel matrix.



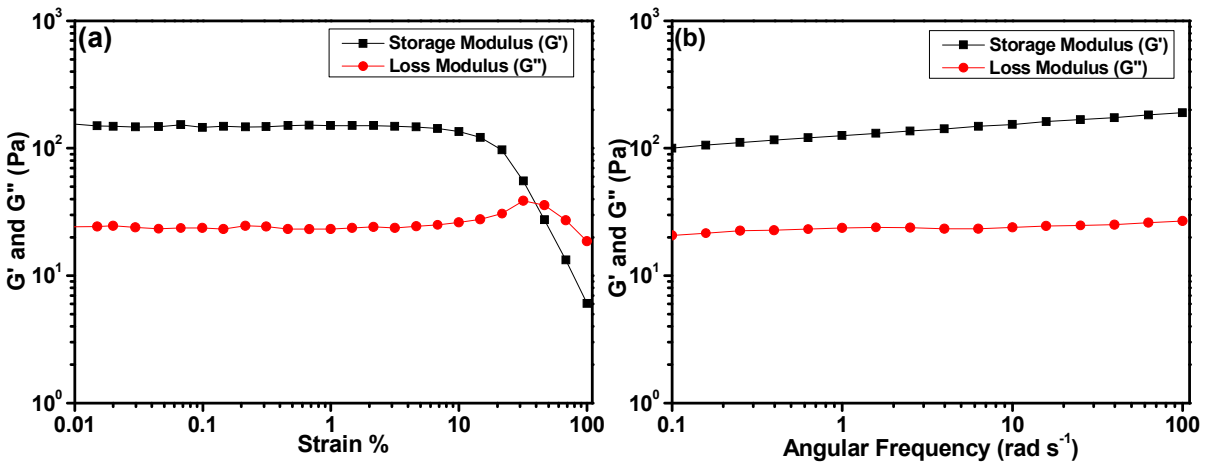
**Fig. S21:** EDX and Mapping analysis of **M<sub>3</sub>G<sub>8</sub>GE(OAc)<sub>2</sub>** showing the presence of C, N, O and Pb inside gel matrix.



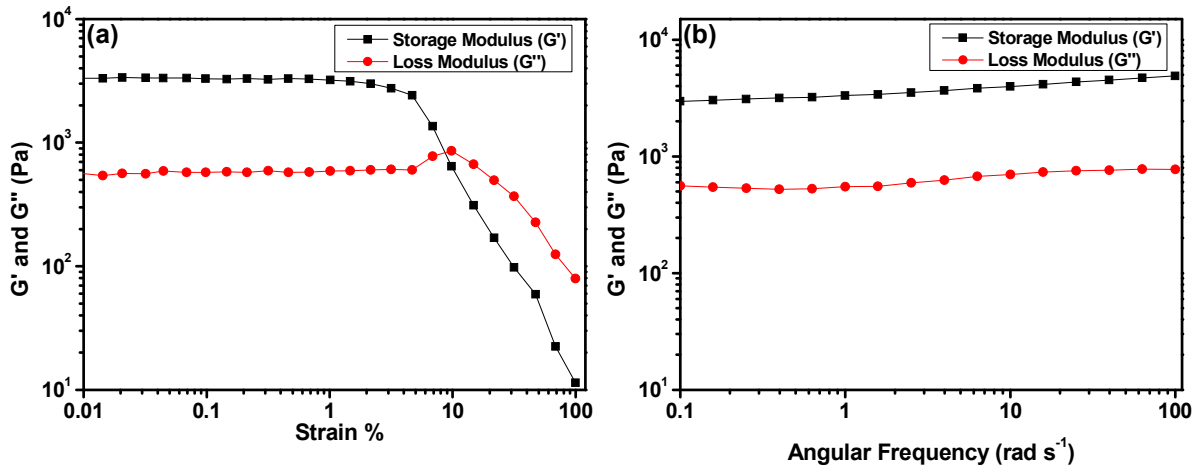
**Fig. S22:** (a) Frequency sweep experiment of organogel **G8GE** at 1:1 molar ratio (0.03: 0.03 mmol) (b) Frequency sweep experiment of organogel **G8GE** at 3: 2 molar ratio (0.03: 0.02 mmol).



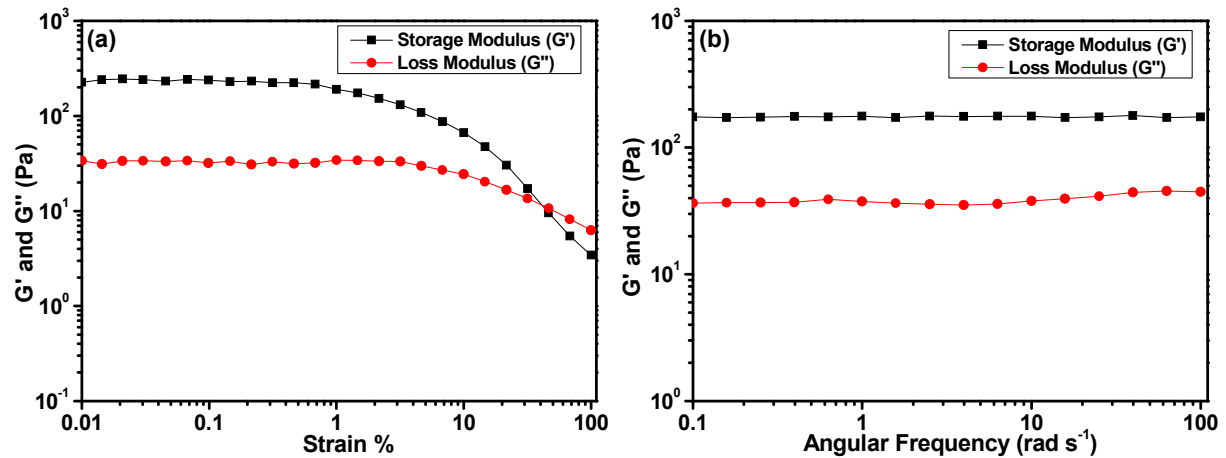
**Fig. S23:** (a) Angular sweep experiment of metallogel **M1G8GECl<sub>2</sub>** (b) Frequency sweep experiment of metallogel **M1G8GECl<sub>2</sub>**.



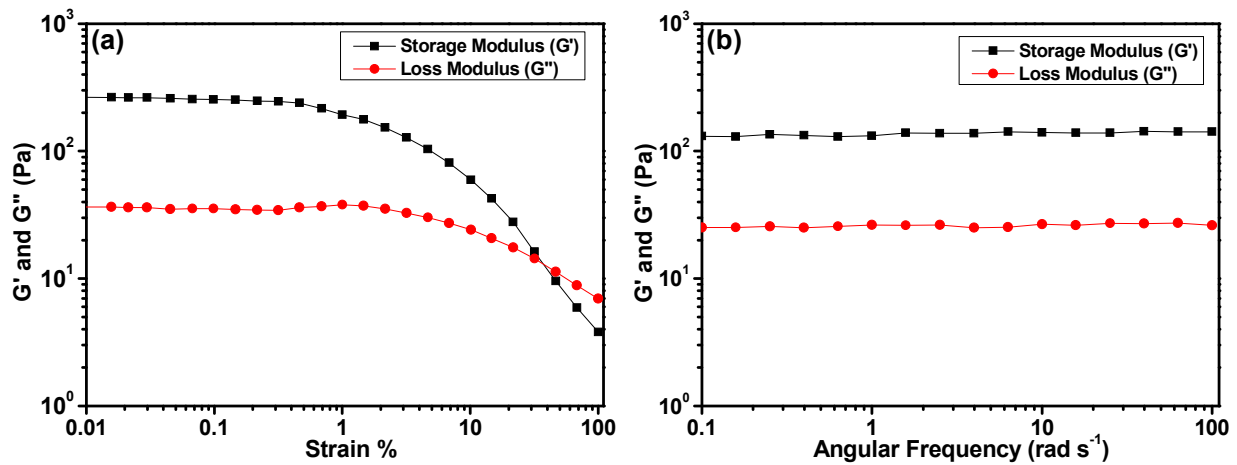
**Fig. S24:** (a) Angular sweep experiment of metallogel **M1G8GE(OAc)<sub>2</sub>** (b) Frequency sweep experiment of metallogel **M1G8GE(OAc)<sub>2</sub>**.



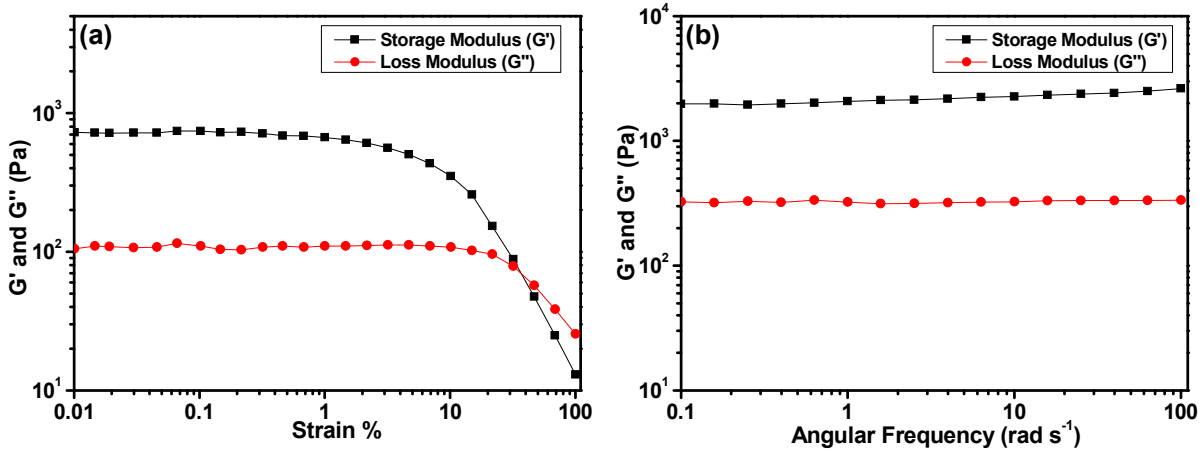
**Fig. S25:** (a) Angular sweep experiment of metalloge **M1G8GESO<sub>4</sub>** (b) Frequency sweep experiment of metalloge **M1G8GESO<sub>4</sub>**.



**Fig. S26:** (a) Angular sweep experiment of metalloge **M2G8GECl<sub>2</sub>** (b) Frequency sweep experiment of metalloge **M2G8GECl<sub>2</sub>**.



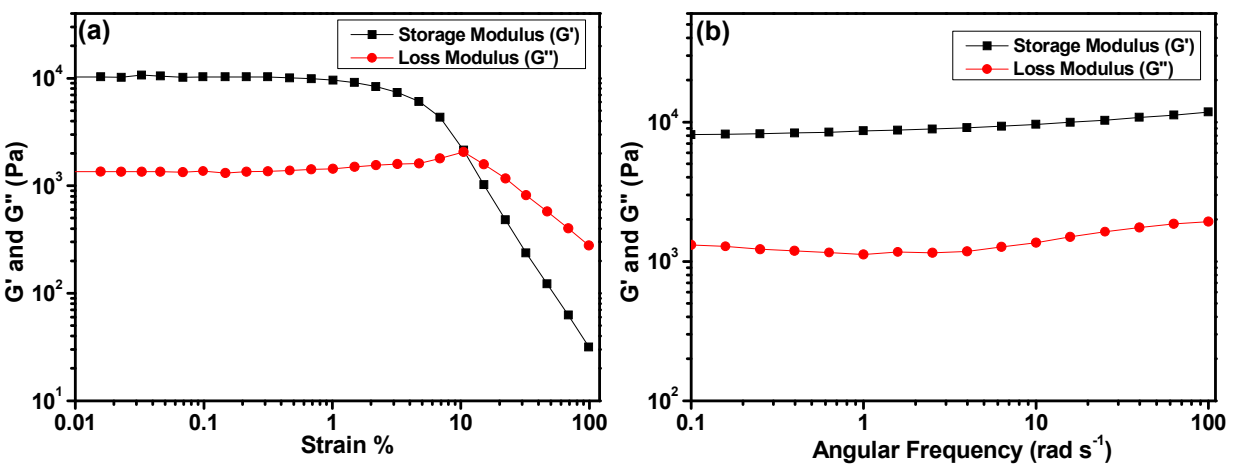
**Fig. S27:** (a) Angular sweep experiment of metalloge **M3G8GECl<sub>2</sub>** (b) Frequency sweep experiment of metalloge **M3G8GECl<sub>2</sub>**.



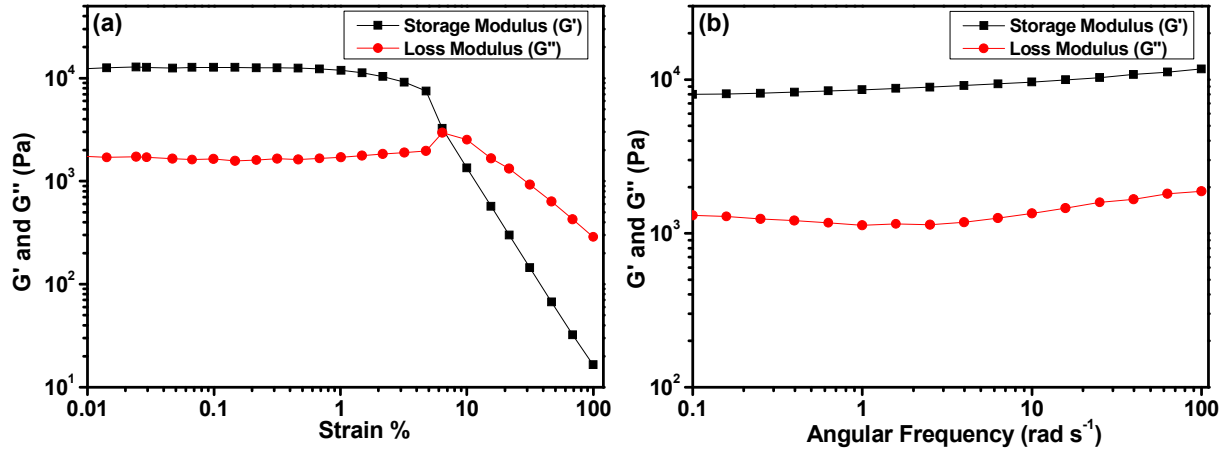
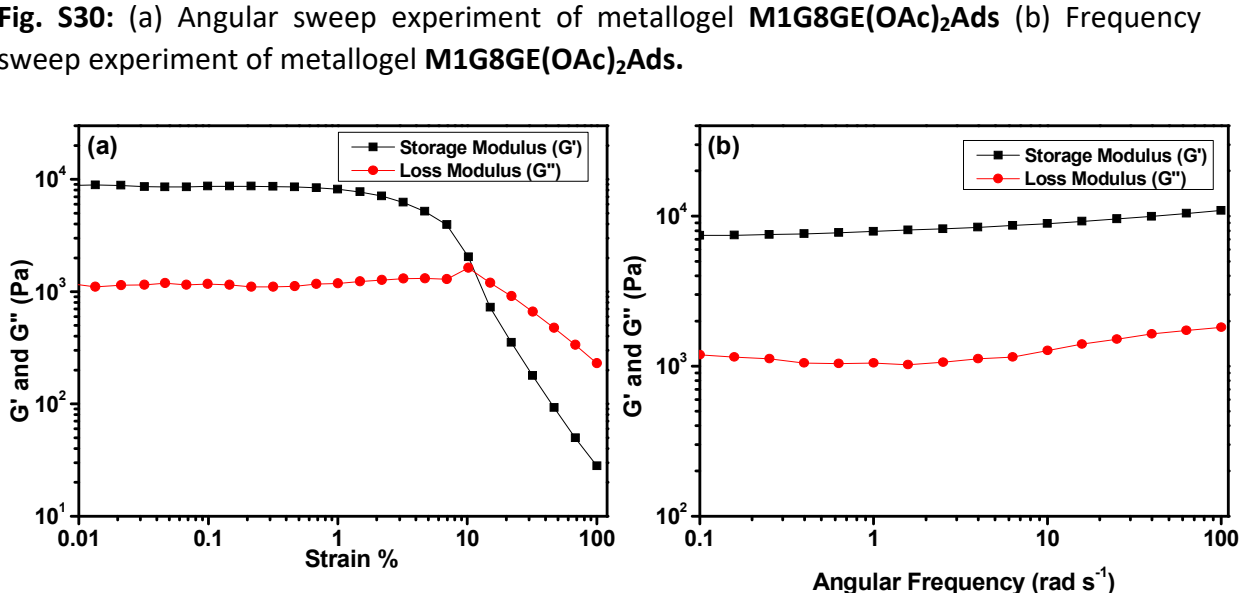
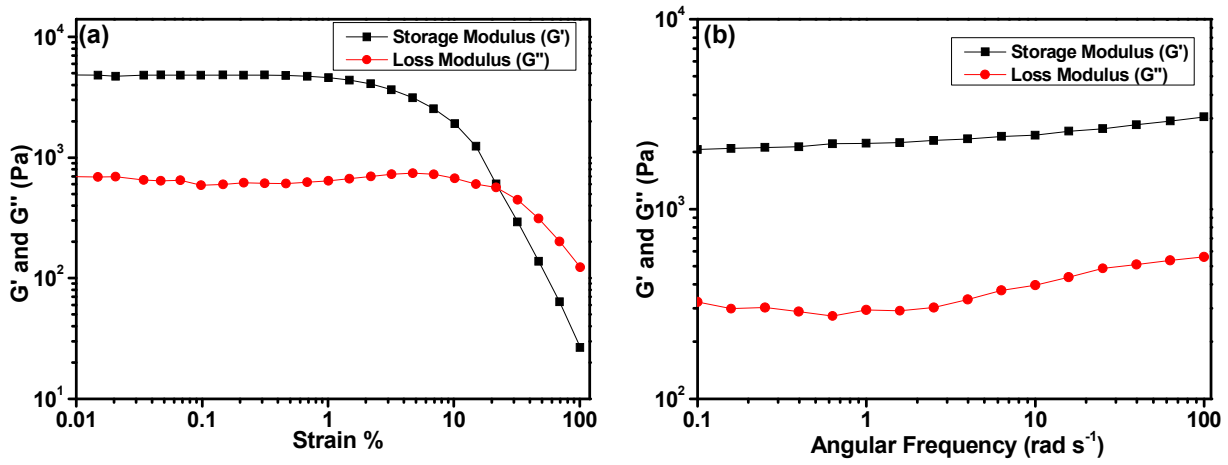
**Fig. S28:** (a) Angular sweep experiment of metallogel **M3G8GESO<sub>4</sub>** (b) Frequency sweep experiment of metallogel **M3G8GESO<sub>4</sub>**.

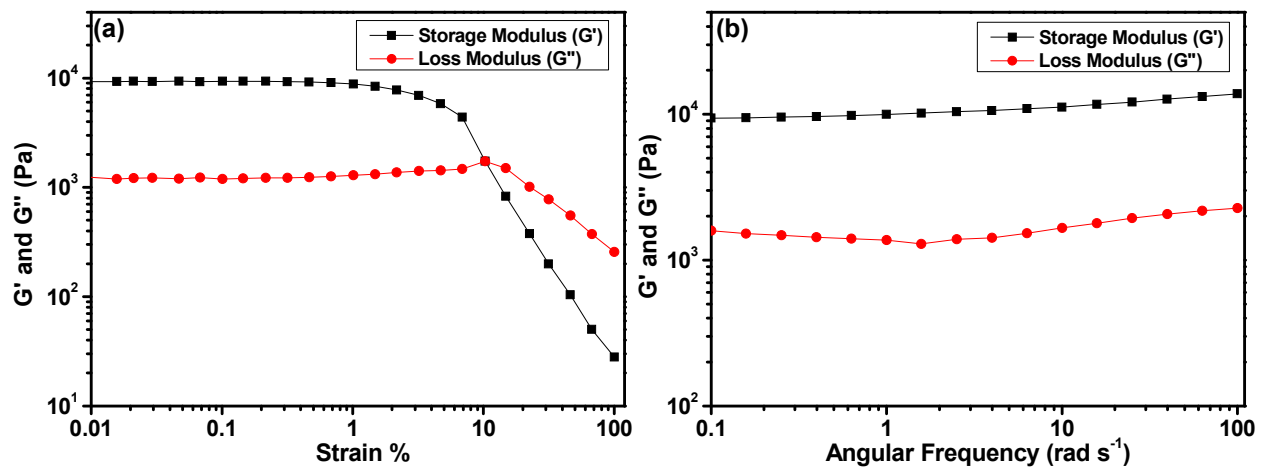
**Table S2:** Storage modulus and loss modulus of metallogels formed by mixing method.

Metallogel	Storage Modulus ( $G'$ )	Loss Modulus ( $G''$ )
<b>M1G8GECl<sub>2</sub></b>	1976 Pa	247 Pa
<b>M1G8GE(OAc)<sub>2</sub></b>	189 Pa	27 Pa
<b>M1G8GESO<sub>4</sub></b>	4838 Pa	792 Pa
<b>M2G8GECl<sub>2</sub></b>	176 Pa	44 Pa
<b>M2G8GE(OAc)<sub>2</sub></b>	Gelatinous Solution	Gelatinous Solution
<b>M2G8GESO<sub>4</sub></b>	Gelatinous Solution	Gelatinous Solution
<b>M3G8GECl<sub>2</sub></b>	140 Pa	26 Pa
<b>M3G8GE(OAc)<sub>2</sub></b>	2646 Pa	338 Pa

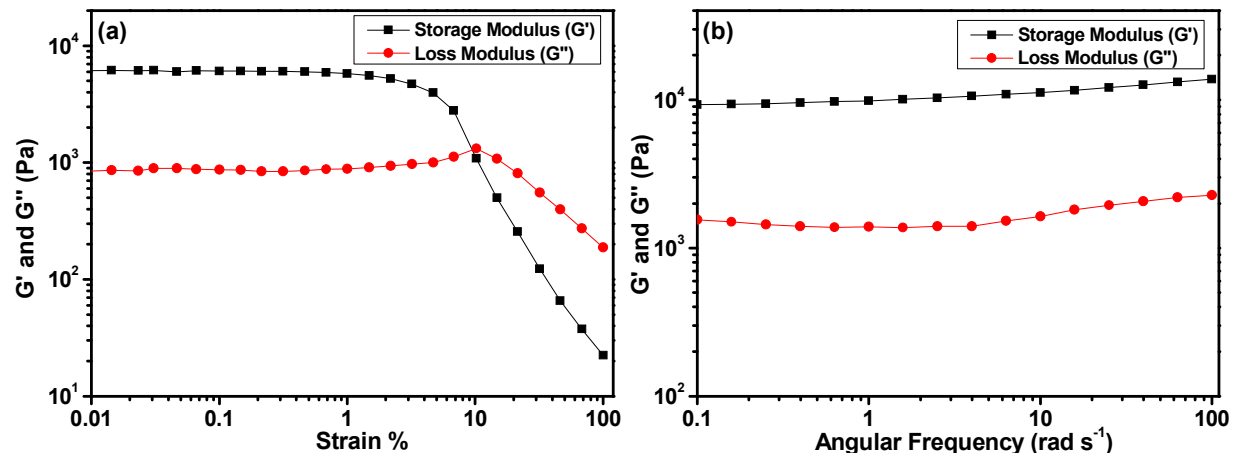


**Fig. S29:** (a) Angular sweep experiment of metallogel **M1G8GECl<sub>2</sub>Ads** (b) Frequency sweep experiment of metallogel **M1G8GECl<sub>2</sub>Ads**.

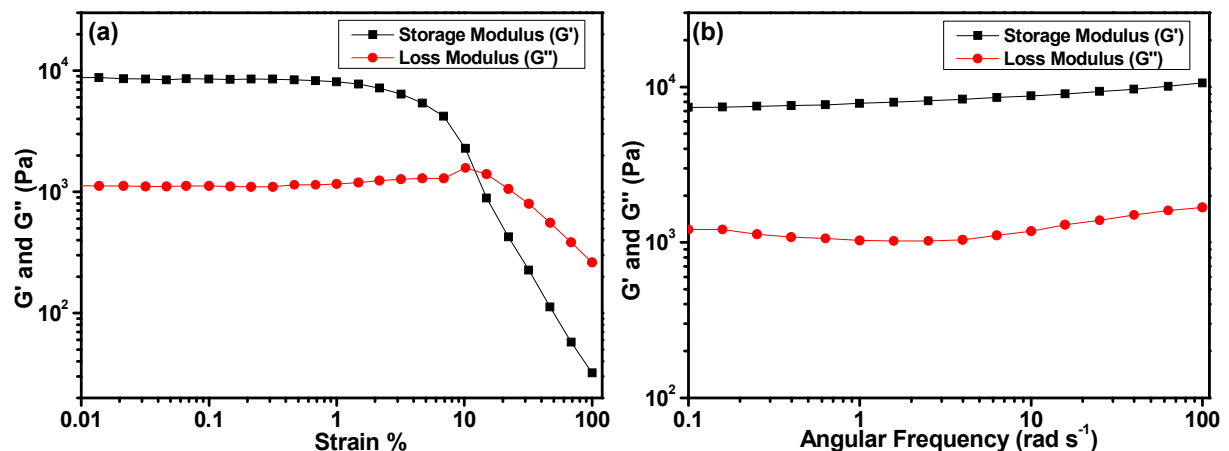




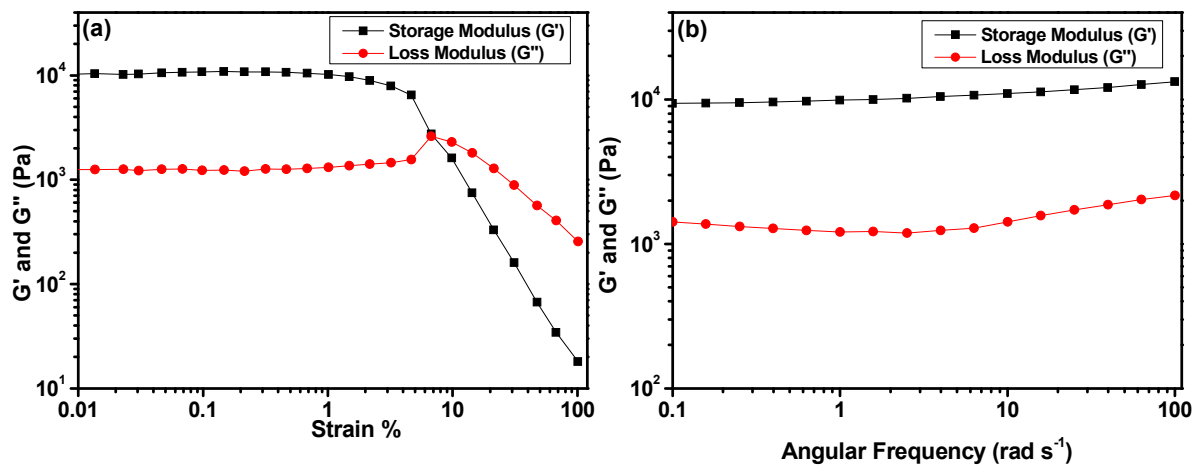
**Fig. S33:** (a) Angular sweep experiment of metallogel **M2G8GE(OAc)<sub>2</sub>Ads** (b) Frequency sweep experiment of metallogel **M2G8GE(OAc)<sub>2</sub>Ads**.



**Fig. S34:** (a) Angular sweep experiment of metallogel **M2G8GESO<sub>4</sub>Ads** (b) Frequency sweep experiment of metallogel **M2G8GESO<sub>4</sub>Ads**.



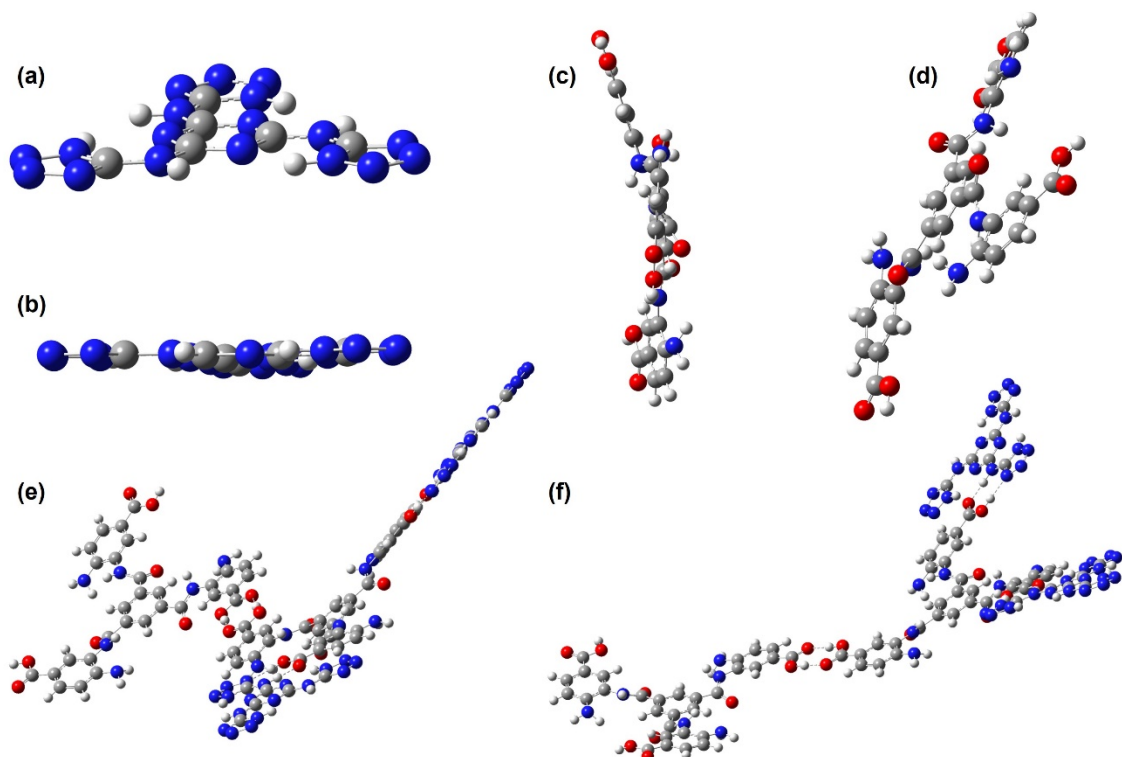
**Fig. S35:** (a) Angular sweep experiment of metallogel **M3G8GECI<sub>2</sub>Ads** (b) Frequency sweep experiment of metallogel **M3G8GECI<sub>2</sub>Ads**.



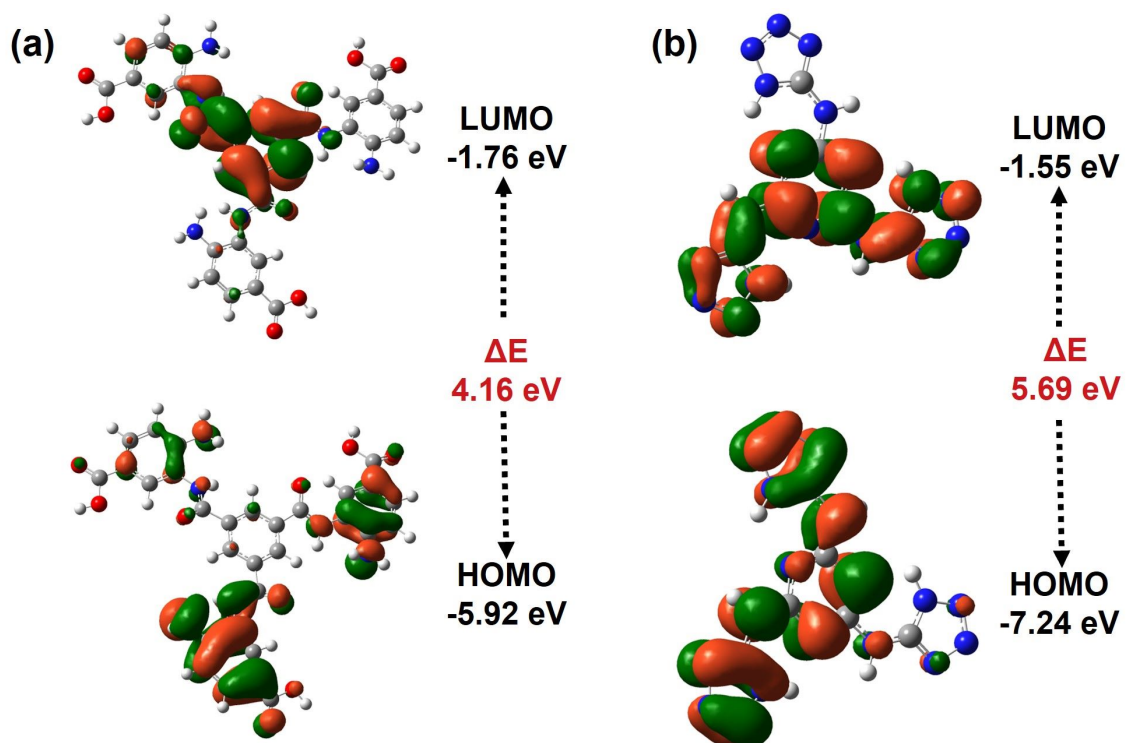
**Fig. S36:** (a) Angular sweep experiment of metallogel **M3G8GE(OAc)<sub>2</sub>Ads** (b) Frequency sweep experiment of metallogel **M3G8GE(OAc)<sub>2</sub>Ads**.

**Table S3:** Storage modulus and loss modulus of metallogels formed by adsorption method.

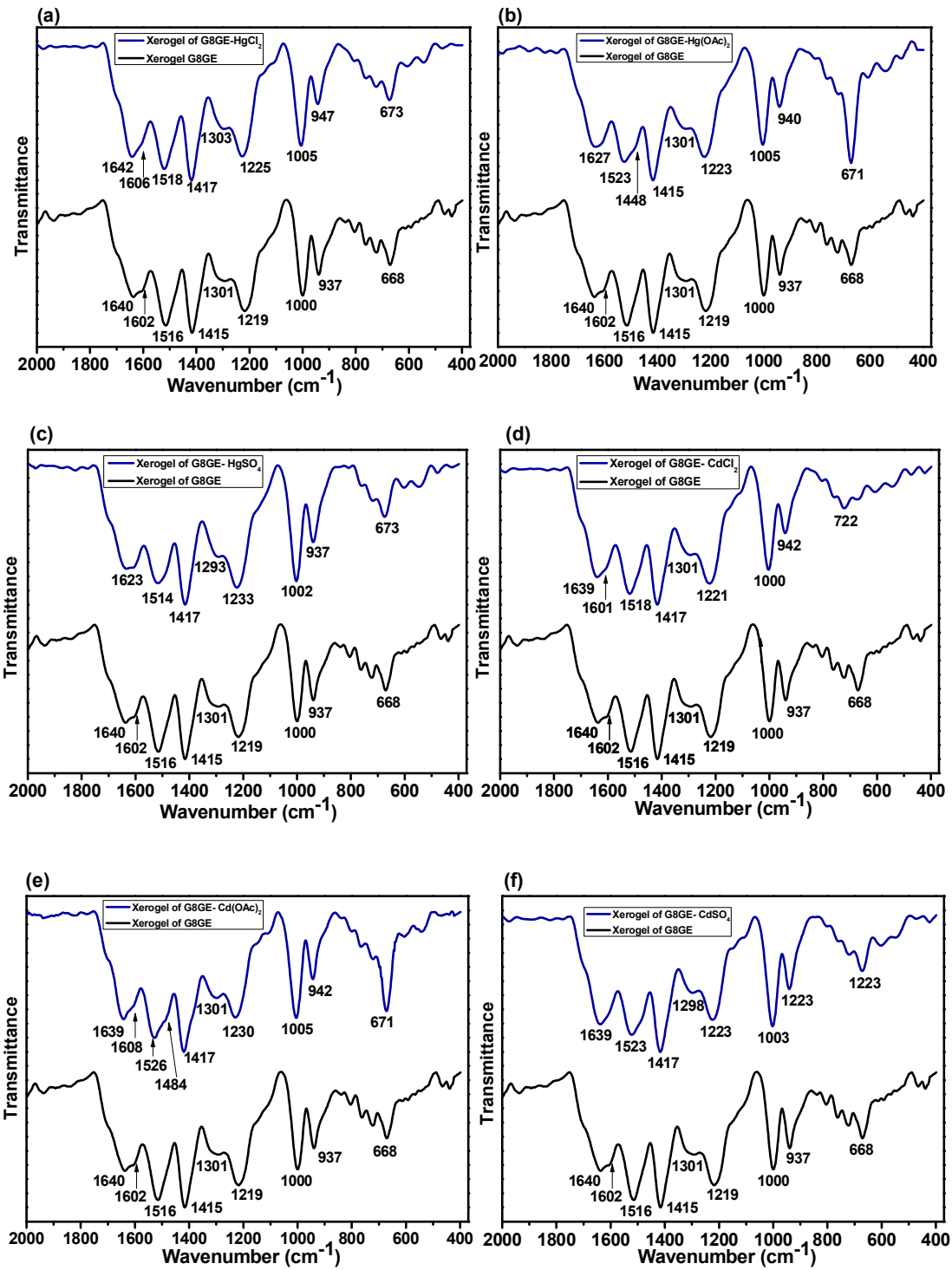
Metallogel	Storage Modulus ( $G'$ )	Loss Modulus ( $G''$ )
<b>M1G8GECl<sub>2</sub>Ads</b>	11730 Pa	1943 Pa
<b>M1G8GE(OAc)<sub>2</sub>Ads</b>	3055 Pa	559 Pa
<b>M1G8GESO<sub>4</sub>Ads</b>	10872 Pa	1803 Pa
<b>M2G8GECl<sub>2</sub>Ads</b>	11830 Pa	1855 Pa
<b>M2G8GE(OAc)<sub>2</sub>Ads</b>	13815 Pa	2291 Pa
<b>M2G8GESO<sub>4</sub>Ads</b>	13635 Pa	2266 Pa
<b>M3G8GECl<sub>2</sub>Ads</b>	10747 Pa	1688 Pa
<b>M3G8GE(OAc)<sub>2</sub>Ads</b>	13119 Pa	2179 Pa



**Fig. S37:** DFT structure showing (a, b) Planarity of **G8** (c, d) Tilted structure of **GE** and (e, f) Less tilted structure of **G8GE** as compared to **GE** after interaction with **G8**.



**Fig. S38:** HOMO-LUMO energy orbitals of (a) **G8** and (b) **GE**.



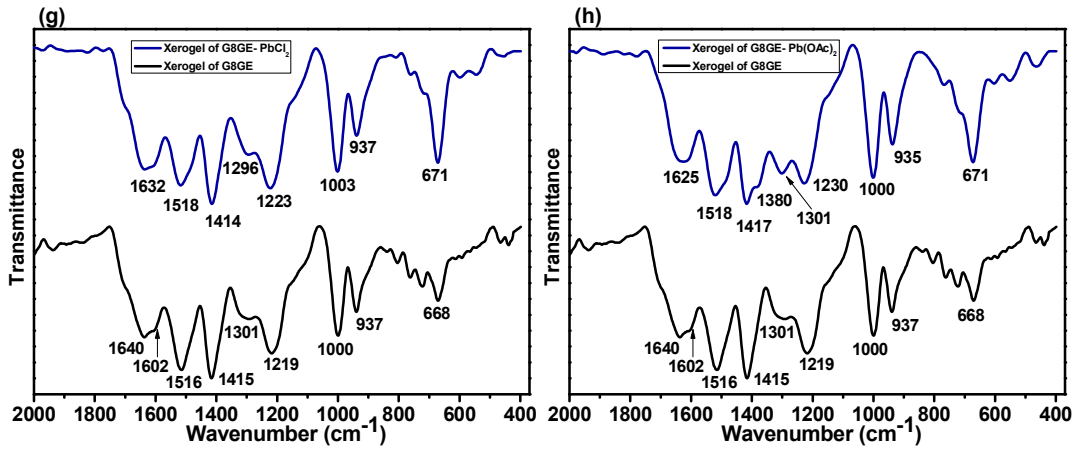


**Fig. 39:** FTIR data analysis of (a) **M1G8GECl<sub>2</sub>** (b) **M1G8GE(OAc)<sub>2</sub>** (c) **M1G8GESO<sub>4</sub>** (d) **M2G8GECl<sub>2</sub>** (e) precipitate of **M2G8GE(OAc)<sub>2</sub>** (f) precipitate of **M2G8GESO<sub>4</sub>** (g) **M3G8GECl<sub>2</sub>** (h) **M3G8GE(OAc)<sub>2</sub>**.

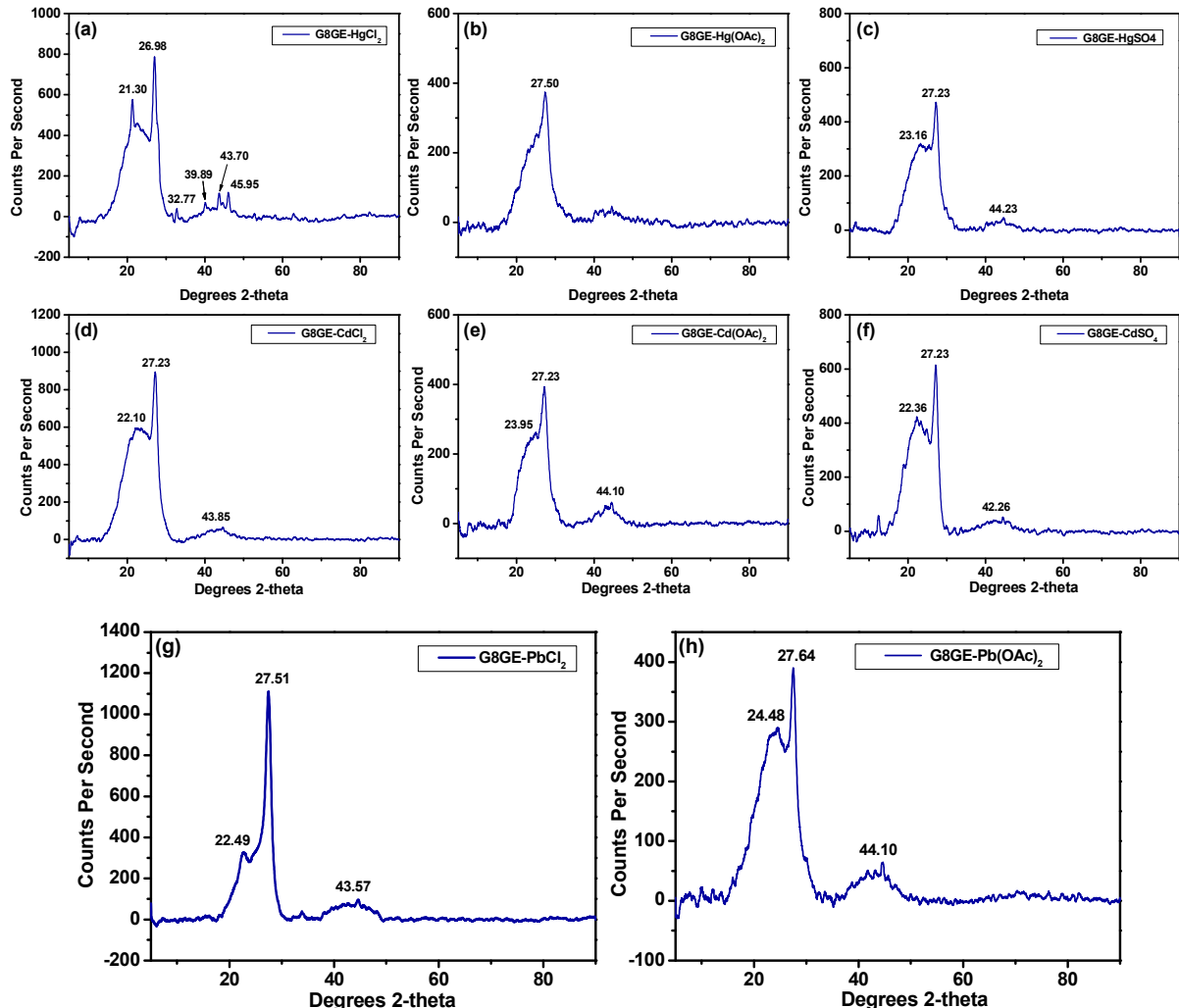


**Fig. S40:** PXRD data of metallogels (a) **M1G8GECl<sub>2</sub>** (b) **M1G8GE(OAc)<sub>2</sub>** (c) **M1G8GESO<sub>4</sub>** (d) **M2G8GECl<sub>2</sub>** (e) precipitate of **M2G8GE(OAc)<sub>2</sub>** (f) precipitate of **M2G8GESO<sub>4</sub>** (g) **M3G8GECl<sub>2</sub>** (h) **M3G8GE(OAc)<sub>2</sub>**.

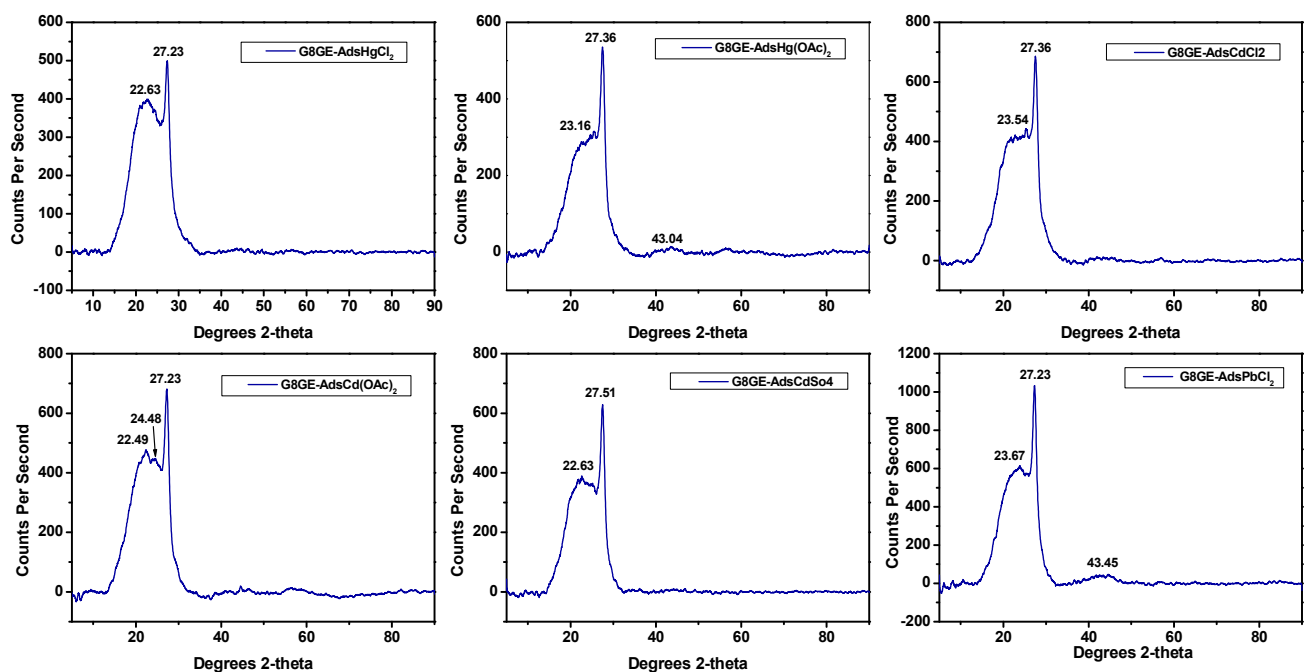


**Fig. S41:** PXRD data of metallogeles (a) M1G8GECl<sub>2</sub> Ads (b) M1G8GE(OAc)<sub>2</sub> Ads (c) M2G8GECl<sub>2</sub> Ads (d) M2G8GE(OAc)<sub>2</sub> Ads (e) M2G8GESO<sub>4</sub> Ads (f) M3G8GECl<sub>2</sub> Ads.

**Table S4:** Optimization of heavy metal removal reaction by xerogel of organogel **G8GE**, analysed by ICP-AES.

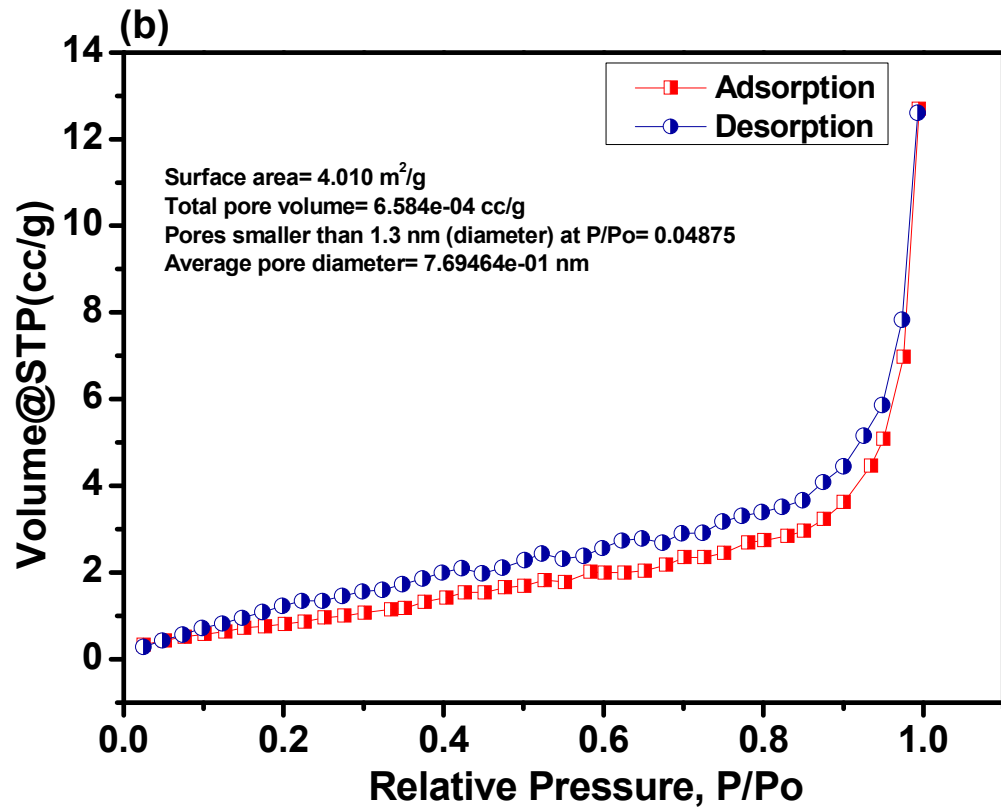
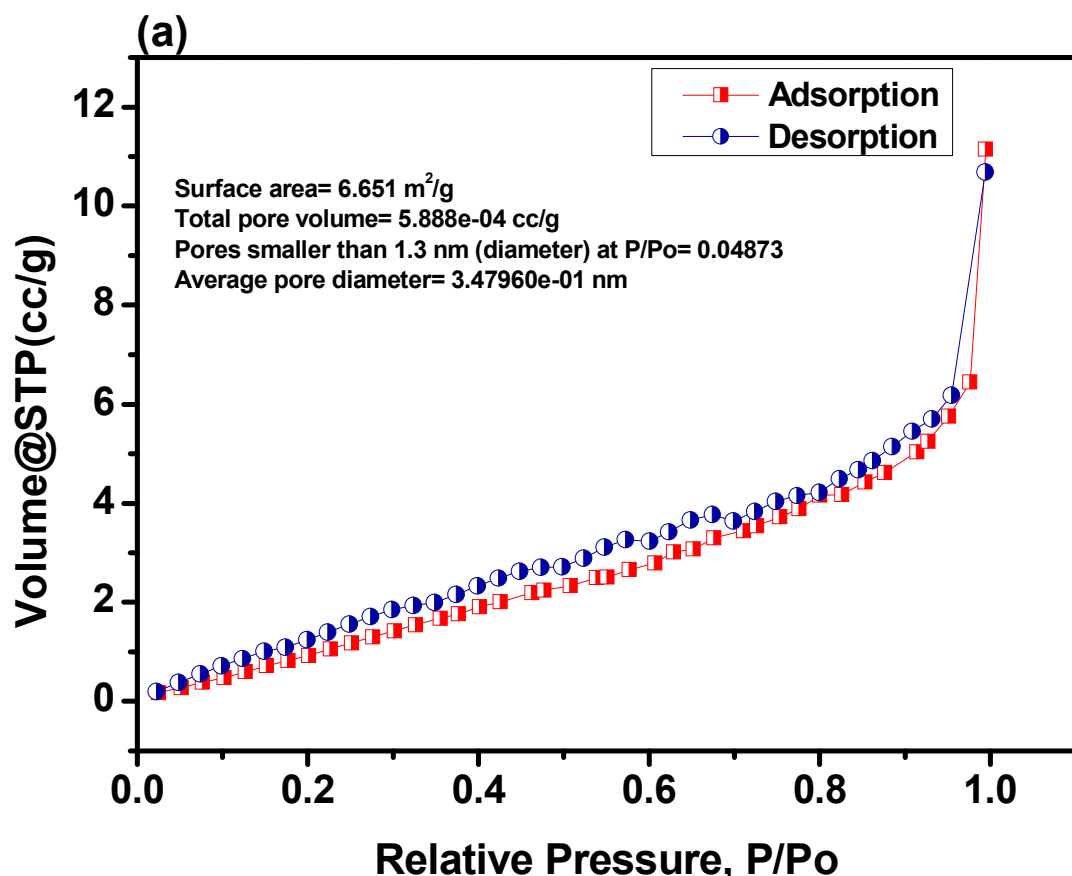
S.No.	Volume of solvent (H <sub>2</sub> O) used	Metal salt and concentration used	Amount of xerogel used	Time for removal operation (hour)	Removal %
1	20 mL water	Hg(OAc) <sub>2</sub> , 1 mM	10 mg	3	57.45
2				6	60.48
3			20 mg	3	72.52
4				6	80.12
5			40 mg	3	90.56
6				6	99.24

**Table S5:** ICP-AES analysis of study of adsorption property of organogel G8GE.

Heavy metal salt	Concentration in ppm before treatment in 20 mL water	Concentration in ppm after treatment by xerogel G8GE (ppm)	Adsorption capacity (q) in (mg/g)	% of heavy metal separation from water
HgCl <sub>2</sub>	271 ppm (1 mM)	118.517	76.24	56.27 %
Hg(CH <sub>3</sub> COO) <sub>2</sub>	318 ppm (1 mM)	2.42	157.79	99. 24 %
HgSO <sub>4</sub>	296 ppm (1 mM)	0.289	147.81	99.90 %
CdCl <sub>2</sub>	201 ppm (1 mM)	96.818	52.09	51.83 %
Cd(CH <sub>3</sub> COO) <sub>2</sub>	266 ppm (1 mM)	3.501	131.25	98.68 %
CdSO <sub>4</sub>	769 ppm (1 mM)	119.437	284.93	84.47%
PbCl <sub>2</sub>	278 ppm (1 mM)	112.033	83	59.70 %
Pb(CH <sub>3</sub> COO) <sub>2</sub>	443 ppm (1 mM)	0.432	221.02	99.90 %

**Table S6:** Adsorption capacity of various gel-based adsorbent.

S. No.	Adsorbent	Adsorbate	Adsorption capacity (q)	References
1	Bi-component supramolecular gel (RQ)	Hg <sup>2+</sup>	59 mg/g	Ref. 1
2	Alginate cryogel of sweet lime-derived activated carbon (SLACC)	Cr <sup>6+</sup> , Cd <sup>2+</sup> , Pb <sup>2+</sup> , Hg <sup>2+</sup> and As <sup>3+</sup>	3.71, 4.22, 20.04, 4.37 and 7.31 mg/g	Ref. 2
3	Xerogel of BTG organogel	Cu <sup>2+</sup> and Hg <sup>2+</sup>	99.02 % and 99.46 % (1 × 10 <sup>-5</sup> M metal salt by 1 mg of xerogel)	Ref. 3
4	G-L organogel	Pb <sup>2+</sup> and Hg <sup>2+</sup>	85.63 % and 99.95 % ( For Pb <sup>2+</sup> it is from 301.5 mg/L to 43.34 mg/L and for Hg <sup>2+</sup> , it is from 24.12 to 0.011 mg/L) with xerogel 1 wt. %in 2mL	Ref. 4
5	Xerogel of G8GE organogel	Chloride, acetate and sulphate salt of Hg <sup>2+</sup> and Cd <sup>2+</sup> , Chloride and acetate of Pb <sup>2+</sup>	76.24, 157.79, 147.81, 52.09, 131.25, 284.93, 83 and 221.02 respectively.	This work



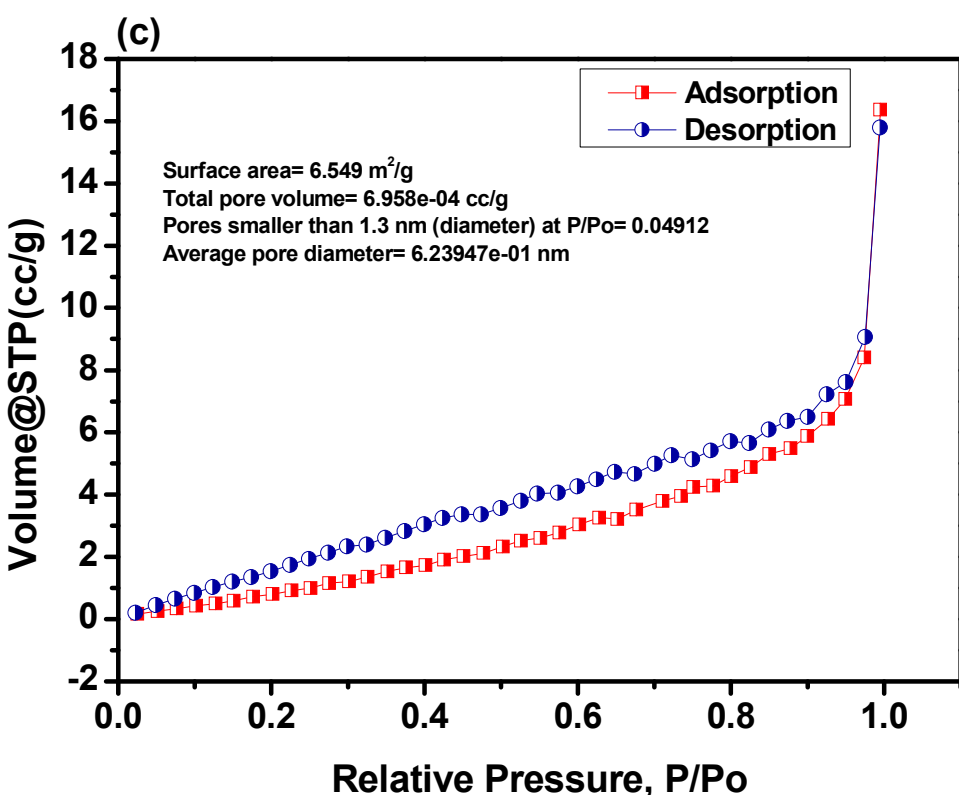


**Fig. S42:** BET analysis data of (a) Xerogel **G8GE** before  $\text{Hg(OAc)}_2$  adsorption (b) After  $\text{Hg(OAc)}_2$  adsorption and (c) after  $\text{Hg(OAc)}_2$  removal from xerogel **G8GE** or recovery of xerogel **G8GE**.

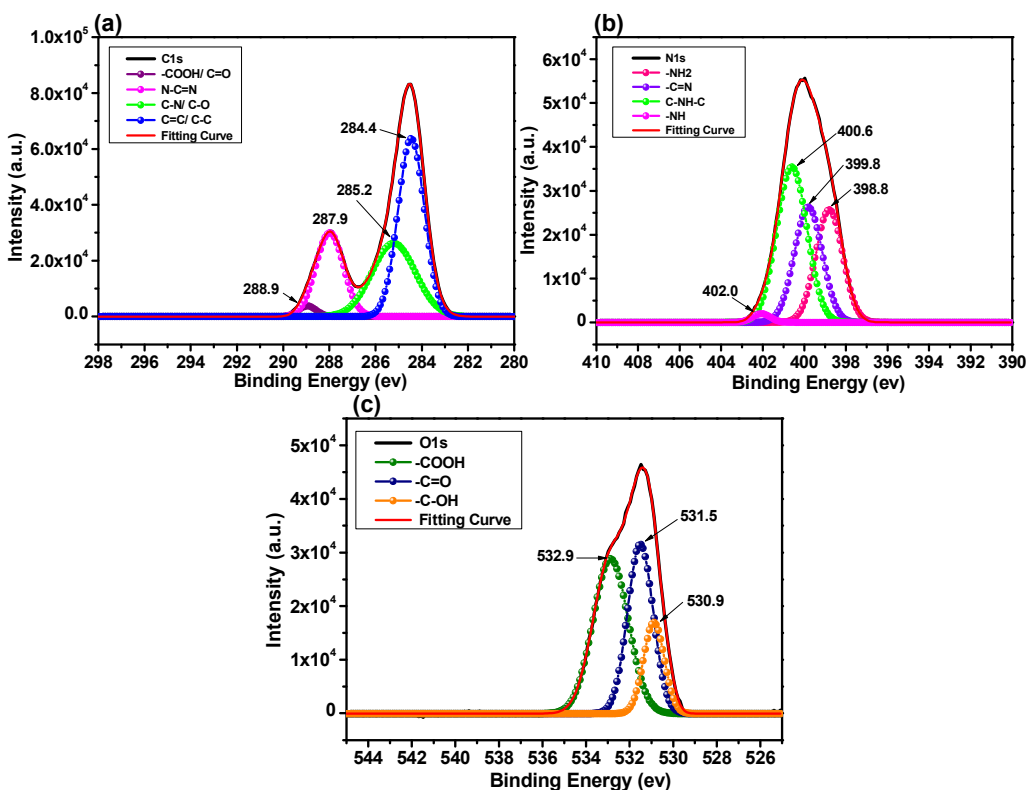


**Fig. S43:** XPS analysis of xerogel **G8GE** showing (a) C1s spectrum (b) N1s spectrum and (c) O1s spectrum.

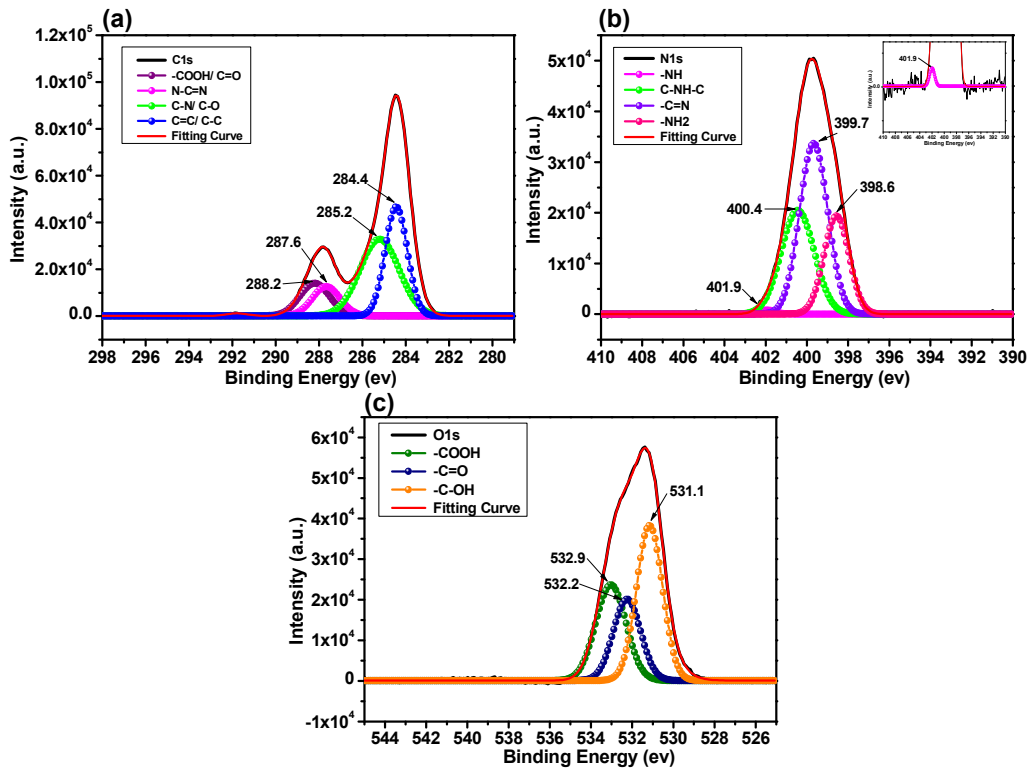


**Fig. S44:** XPS analysis of xerogel **mtG8GE** showing (a) C1s spectrum (b) N1s spectrum and (c) O1s spectrum.

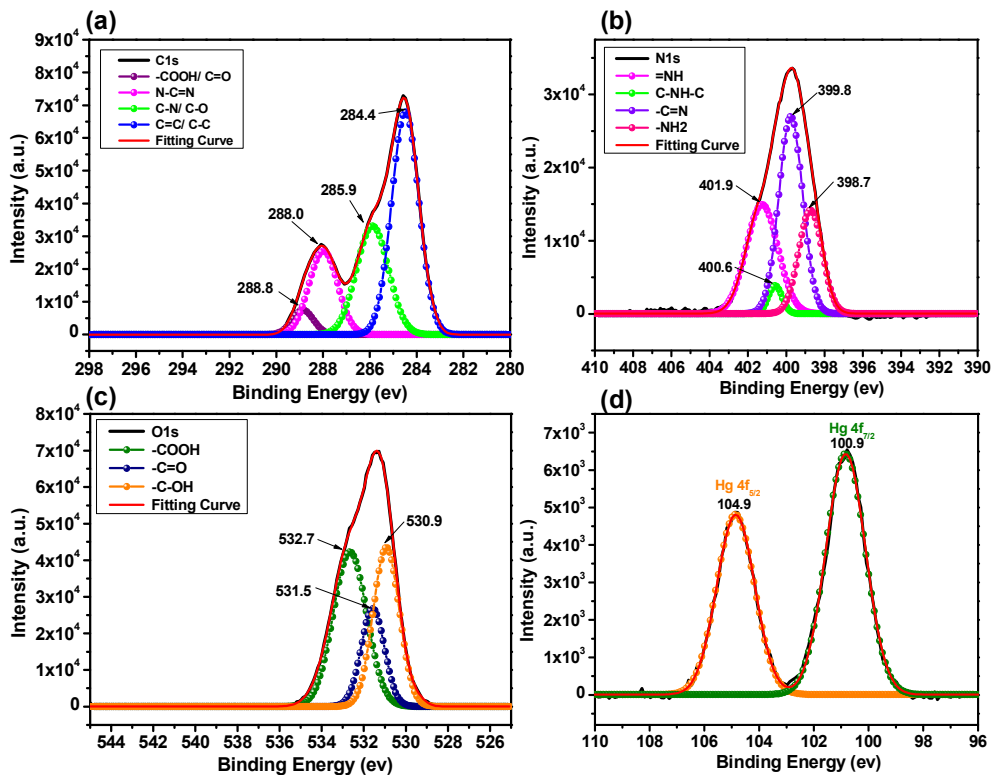


**Fig. S45:** XPS analysis of xerogel **mrG8GE** showing (a) C1s spectrum (b) N1s spectrum and (c) O1s spectrum and (d) Hg 4f spectrum.

**Table S7:** XPS peaks position of various groups for **G8GE**, **mtG8GE** and recovered **mrG8GE**.

Groups or Element present	Xerogel <b>G8GE</b> Binding Energy (eV)	<b>mtG8GE</b> Binding Energy (eV)	<b>mrG8GE</b> Binding Energy (eV)
-COOH/ C=O	<b>288.9</b>	<b>288.2</b>	<b>288.8</b>
N-C=N	<b>287.9</b>	<b>287.6</b>	<b>288.0</b>
C-N/ C-O	<b>285.2</b>	<b>285.2</b>	<b>285.9</b>
C=C/ C-C	<b>284.4</b>	<b>284.4</b>	<b>284.4</b>
-NH	<b>402.0</b>	<b>401.9</b>	<b>401.9</b>
C-NH-C	<b>400.6</b>	<b>400.4</b>	<b>400.6</b>
-C=N	<b>399.8</b>	<b>399.7</b>	<b>399.8</b>
-NH <sub>2</sub>	<b>398.8</b>	<b>398.6</b>	<b>398.7</b>
-COOH	<b>532.9</b>	<b>532.9</b>	<b>532.7</b>
C=O	<b>531.5</b>	<b>532.2</b>	<b>531.5</b>
C-OH	<b>530.9</b>	<b>531.1</b>	<b>530.9</b>
Hg <sup>2+</sup> (Hg 4f <sub>7/2</sub> )	-	<b>100.9</b>	<b>100.9</b>
Hg <sup>2+</sup> (Hg 4f <sub>5/2</sub> )	-	<b>104.9</b>	<b>104.9</b>

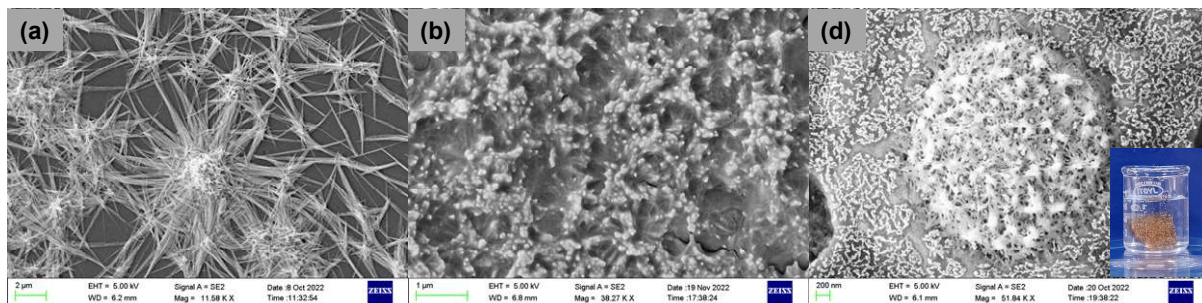


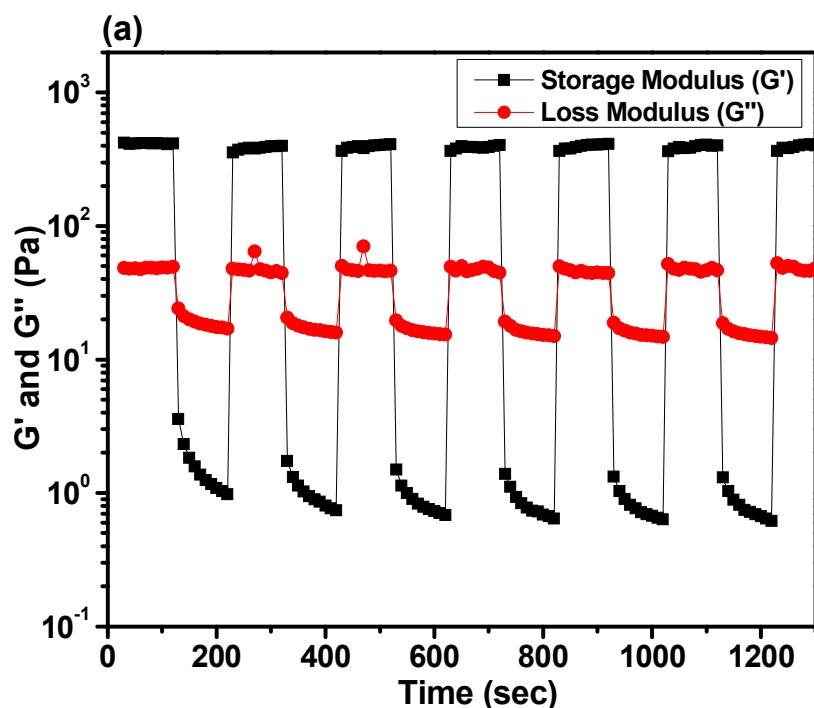
**Fig. S46:** FE-SEM images of (a) **M1G8GECl<sub>2</sub>** gel by mixing (b) **M1G8GECl<sub>2</sub>Ads** by adsorption (c) **M1G8GECl<sub>2</sub>Ads** when **G8GE** inserted inside the aqueous solution of HgCl<sub>2</sub>.

**Table S8:** Recyclability of xerogel **G8GE** for heavy metal separation.

Concentration of $\text{Hg}(\text{CH}_3\text{COO})_2$ in ppm before treatment (20 mL water)	Concentration in ppm after treatment by xerogel G8GE (ppm)	Removal % from water
318 ppm (1 mM)	2.514	99.21
318 ppm (1 mM)	5.092	98.39
318 ppm (1 mM)	5.271	98.34
318 ppm (1 mM)	6.003	98.11
318 ppm (1 mM)	8.311	97.39

**Table S9:** Water remediation at different pH by xerogel **G8GE**.

Concentration of $\text{Hg}(\text{CH}_3\text{COO})_2$ in ppm before treatment (20 mL water)	pH of contaminated water system	Concentration in ppm after treatment by xerogel G8GE (ppm)	Removal % from water
318 ppm (1 mM)	3	87.876	72.36
318 ppm (1 mM)	5.4	2.405	99.24
318 ppm (1 mM)	7	7.338	97.69
318 ppm (1 mM)	10	5.514	98.26



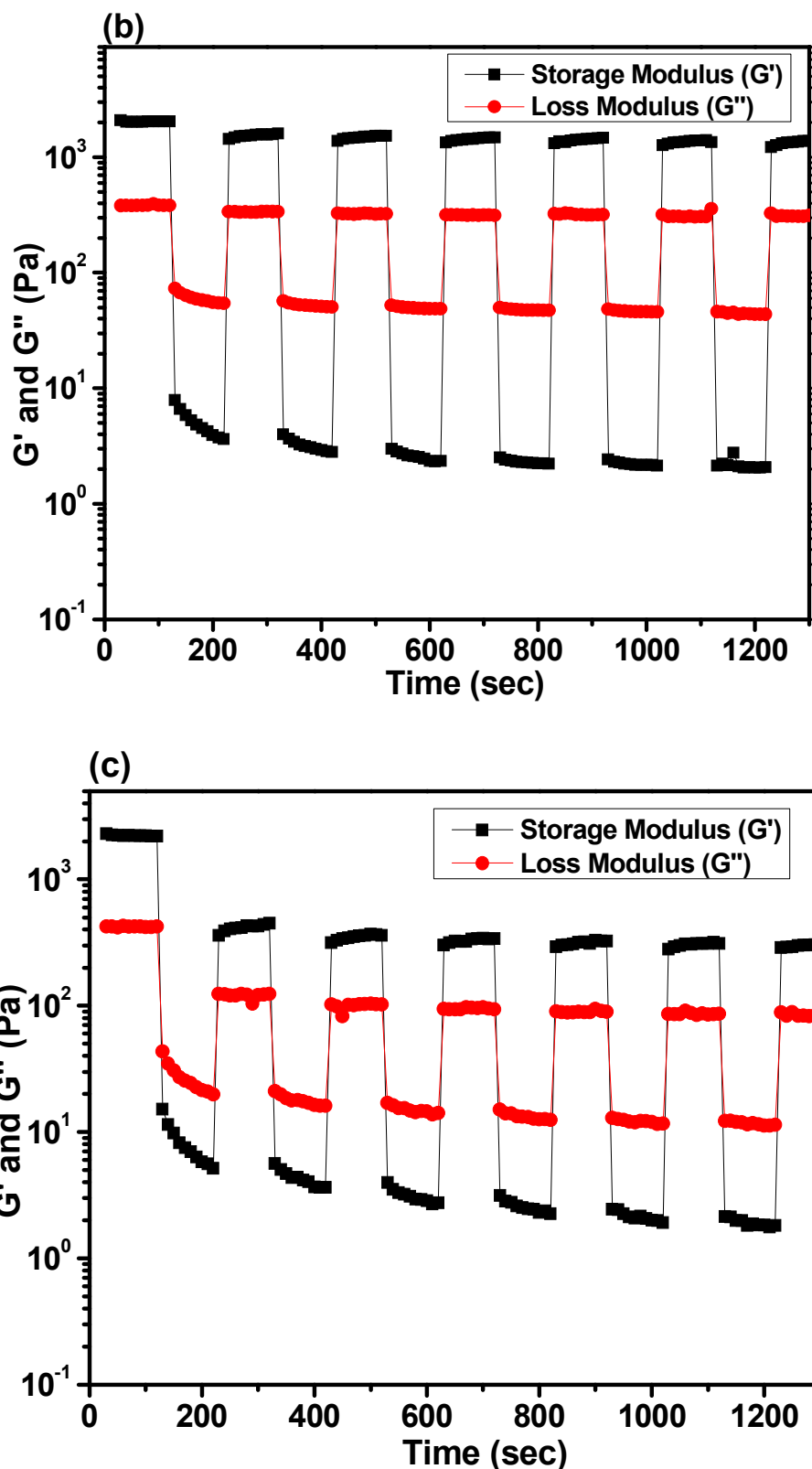


**Fig. S47:** Time oscillation sweep experiment of organogel **G8GE** at (a) 0.02: 0.02 mmol (b) 0.03: 0.03 mmol and (c) 0.04: 0.04 mmol.

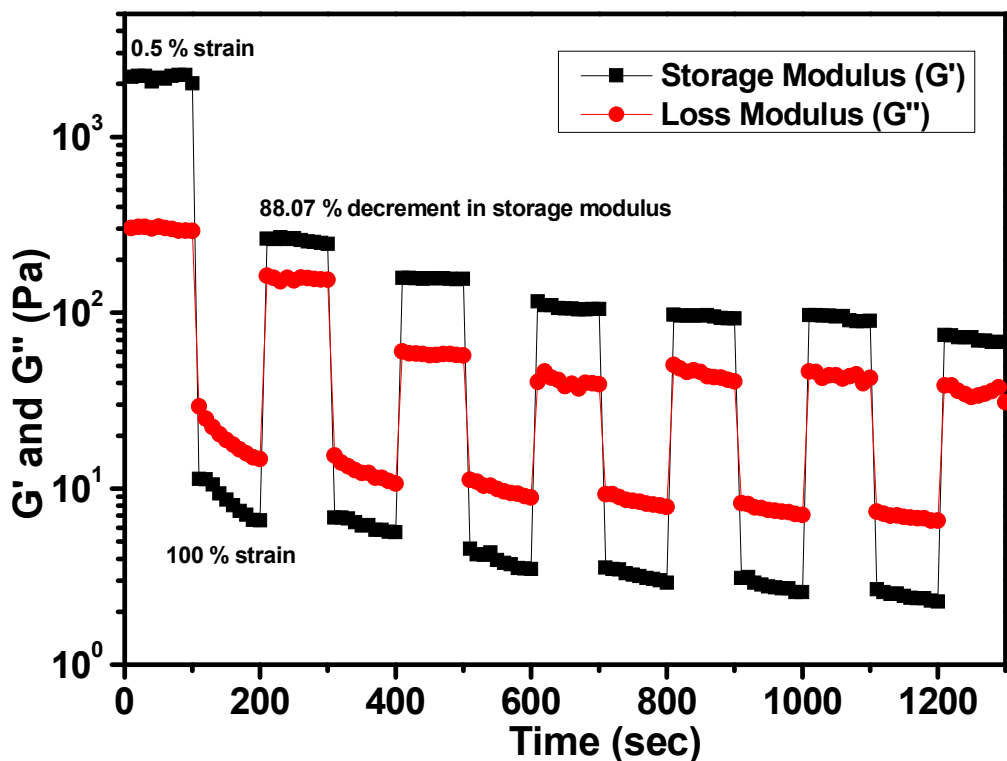


Fig. S48: Time oscillation sweep experiment of metallogel **M3G8GECl<sub>2</sub>**.

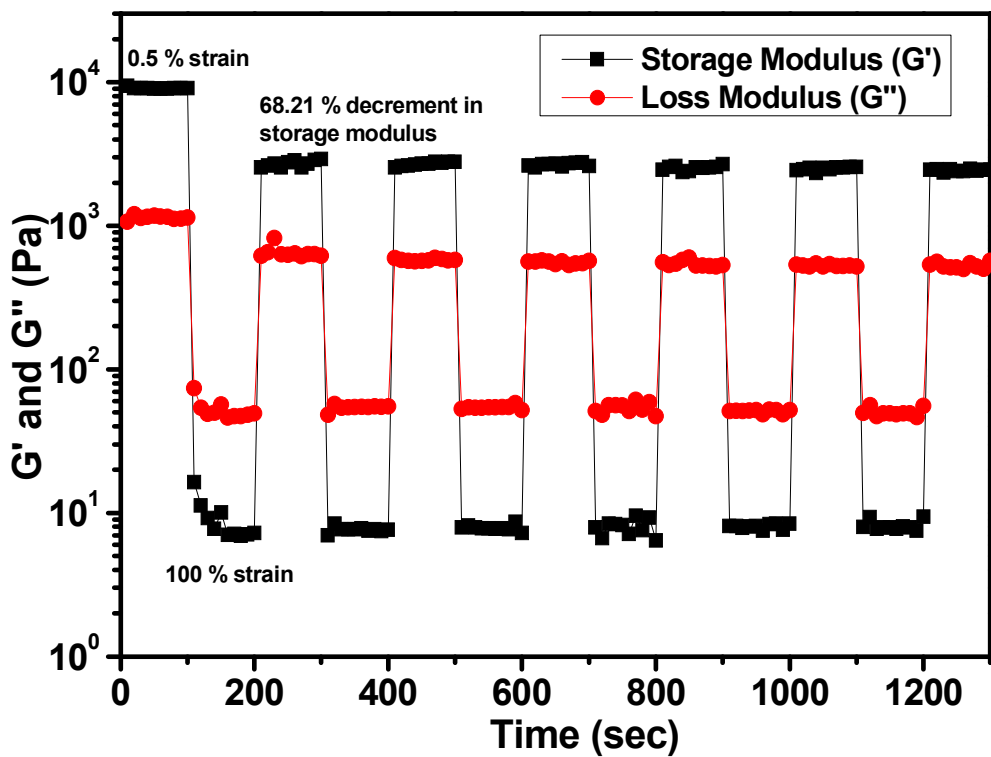
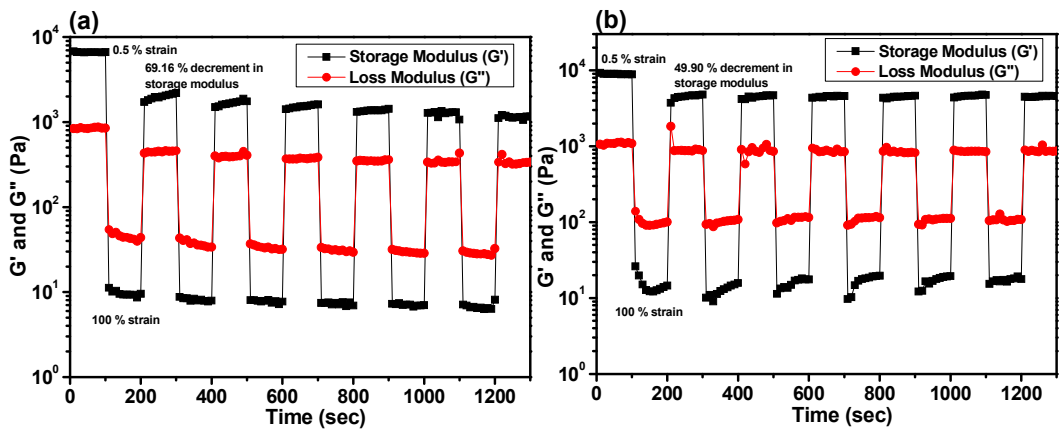
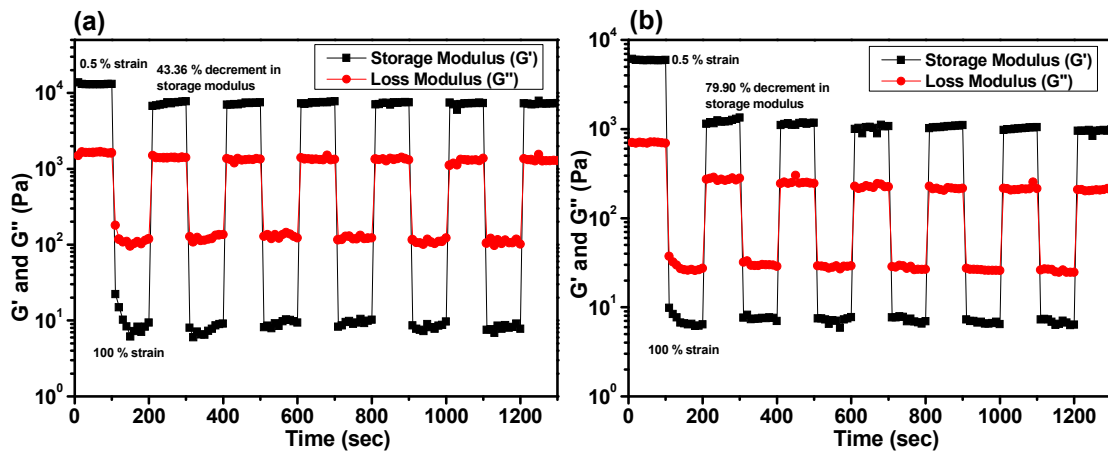


Fig. S49: Time oscillation sweep experiment of metallogel **M2G8GECl<sub>2</sub>Ads**.



**Fig. S50:** Time oscillation sweep experiment of metallogele (a) **M2G8GE(OAc)<sub>2</sub>Ads** and (b) **M2G8GESO<sub>4</sub>Ads**.



**Fig. S51:** Time oscillation sweep experiment of metallogele (a) **M3G8GECl<sub>2</sub>Ads** and (b) **M3G8GE(OAc)<sub>2</sub>Ads**.

**Table S10.** Intermolecular H-bond binding energies of individual sites along with the associated bond lengths of structure **G8GE**.

Binding Site	H-bond length (Å)	$\rho(r_{BCP})$ (a.u.)	HBE (kcal/mol)
O-H...O	1.66	0.0497	-10.33
O-H...O	1.66	0.0497	-10.34
O-H...N	1.86	0.0367	-7.44
O-H...N	1.86	0.0368	-7.46
N-H...O	1.70	0.0466	-9.65
N-H...O	1.70	0.0466	-9.66

**Table S11.** Cartesian coordinates of **GE**.

69

Energy = -2163.413966 Hartree

C	-1.19846001	0.73221939	0.55276116
C	0.02869176	1.39738300	0.56213802
C	1.23003830	0.67766094	0.55260126
C	1.19265187	-0.71858676	0.56012894
C	-0.03149061	-1.39932539	0.55113776
C	-1.22115608	-0.66837765	0.55842979
H	0.09482226	2.47894230	0.61111845
H	2.09676942	-1.31610398	0.60662826
H	-2.19116349	-1.15159696	0.60271265
C	-2.53040615	1.43298728	0.59024847
C	2.50319919	1.48026541	0.58766266
C	0.02672127	-2.90351111	0.58828944
H	-1.69591308	3.06402567	-0.32700222
H	3.48836622	-0.05008641	-0.35052830
H	-1.79486736	-2.99561167	-0.34384610
O	-3.53239696	0.86264417	1.02043008
O	2.51412792	2.62875394	1.02920696
O	1.01880192	-3.48687147	1.02417157
C	-3.67362612	3.56646183	0.01825512
C	-4.94035382	3.08690831	-0.29865477
C	-3.46068302	4.95505480	0.21597418
C	-6.02112368	3.97076342	-0.43468672
H	-5.08282387	2.02479357	-0.43534854
C	-4.54838969	5.83238796	0.04587756
C	-5.80695046	5.34856871	-0.27196254
H	-4.39162436	6.89825656	0.18773794
H	-6.64446209	6.02871452	-0.38427905
C	4.92117952	1.39886617	0.00186529
C	5.14931034	2.74147218	-0.28165803
C	6.01048431	0.50387486	0.16070418
C	6.45866579	3.22388696	-0.42477201
H	4.30655347	3.40904848	-0.38841409
C	7.31677893	0.99635421	-0.01750844
C	7.53749157	2.33375664	-0.30392747
H	8.15565912	0.31476730	0.09308936
H	8.54788170	2.71038291	-0.42269269
C	-1.25132415	-4.95943801	0.01454531
C	-2.56626639	-5.46187043	0.19459111
C	-0.20215316	-5.82343438	-0.28090611
C	-2.78691305	-6.84189881	0.02567421
C	-0.43242739	-7.20047990	-0.41412560
H	0.79330722	-5.42166667	-0.40347363
C	-1.73781901	-7.69659024	-0.27157829
H	-3.79237242	-7.23349374	0.15244468
H	-1.91225248	-8.76140573	-0.38295918
N	-2.54061117	2.71611234	0.11108099

N	3.61582580	0.85010705	0.09618788
N	-1.07672698	-3.55354985	0.10268612
N	-2.18885498	5.42512489	0.50559506
H	-2.14854878	6.39616001	0.79387656
H	-1.63683265	4.83785119	1.12171081
N	-3.60892083	-4.58824108	0.46447757
H	-4.47681386	-5.03391113	0.74009931
H	-3.38189235	-3.81753399	1.08386301
N	5.76930442	-0.83685005	0.42136554
H	6.58858045	-1.37483920	0.67989169
H	4.99724589	-1.02457113	1.05250428
C	-7.38188170	3.50139610	-0.76107190
O	-8.35423701	4.22567990	-0.91309939
O	-7.47136060	2.15255980	-0.87750096
H	-8.40105968	1.95039289	-1.09269482
C	6.74356996	4.64290164	-0.71580212
O	7.85962324	5.11389602	-0.87680826
O	5.62698998	5.40969911	-0.79477948
H	5.92315514	6.31814743	-0.99063721
C	0.65532893	-8.15091367	-0.71756123
O	0.51133837	-9.35519420	-0.86687932
O	1.87198729	-7.55939426	-0.82097735
H	2.51305501	-8.26623023	-1.02367954

**Table S12.** Cartesian coordinates of **G8**.

30

Energy = -1217.738870 Hartree

C	-1.21535050	-0.45363285	0.00000422
C	1.00077919	-0.82616842	-0.00000089
C	0.21537843	1.27937668	-0.00001944
N	1.29445634	0.47734839	-0.00001501
N	-1.06028443	0.88191256	-0.00000903
N	-0.23333181	-1.35970545	0.00000765
H	1.45750405	2.89693034	-0.00004038
H	-3.23673369	-0.18562011	0.00000489
H	1.78025422	-2.71064685	0.00001968
C	-0.43229902	3.64706277	-0.00002452
N	-1.77192724	3.53584929	-0.00000207
H	-2.32050158	2.68258413	0.00001786
C	-2.94288617	-2.19764829	0.00002517
N	-2.17720375	-3.30241305	0.00003900
H	-1.16400359	-3.35118725	0.00004321
C	3.37514475	-1.44933687	-0.00000462
N	3.94865196	-0.23366423	-0.00002590
H	3.48364934	0.66788400	-0.00004194
N	2.02973759	-1.72823997	0.00000503
N	-2.51111901	-0.89334606	0.00001080
N	0.48204458	2.62151062	-0.00002832

N	-0.11085780	4.93340497	-0.00003809
N	-1.29798669	5.59703553	-0.00002258
N	-2.30170728	4.78205726	-0.00000139
N	-4.21779186	-2.56193236	0.00003046
N	-4.19944401	-3.92190063	0.00004837
N	-2.99192505	-4.38404027	0.00004962
N	4.32844276	-2.37094191	0.00000747
N	5.49678629	-1.67469416	-0.00000696
N	5.29277809	-0.39793515	-0.00003232

**Table S13.** Cartesian coordinates of **2GE-2G8 (G8GE)**.

198

Energy = -6762.402264 Hartree

C	15.66640983	-2.02490993	0.20242577
C	14.38171527	-1.62059262	0.57047069
C	14.04557966	-0.26134741	0.61166582
C	15.01742918	0.69309369	0.30485513
C	16.31078690	0.30201333	-0.06474111
C	16.63121680	-1.05649365	-0.10275531
H	13.62051544	-2.33424720	0.86678293
H	14.81894157	1.75699772	0.37400013
H	17.63292493	-1.40335896	-0.33243728
C	16.10881778	-3.46320766	0.16576719
C	12.64347236	0.07776183	1.04279347
C	17.29812290	1.40274929	-0.34774425
H	14.19271342	-4.03186566	-0.27486556
H	12.73685965	1.82089448	-0.02929387
H	18.32547195	0.15395330	-1.60418552
O	17.29342354	-3.76390595	0.30980829
O	11.98449629	-0.70941573	1.72148305
O	17.14363463	2.52708770	0.12814428
C	15.26987022	-5.78946935	-0.13441296
C	16.40388325	-6.38636499	-0.67592073
C	14.18415911	-6.58633843	0.31336846
C	16.48234934	-7.78181884	-0.79577680
H	17.22420261	-5.76320586	-1.00085918
C	14.26547498	-7.98233061	0.15694574
C	15.39596655	-8.57073983	-0.38691647
H	13.43427045	-8.59811888	0.48935252
H	15.45911210	-9.64888138	-0.48830186
C	10.87094099	1.81565790	0.85879390
C	9.73969052	1.01079357	0.93556339
C	10.75546641	3.22609706	0.96966265
C	8.47083820	1.58347742	1.10999219
H	9.84618242	-0.06162325	0.86152945
C	9.47248321	3.78724137	1.11090924
C	8.34856847	2.98026344	1.18087450
H	9.37615724	4.86669115	1.18710182

H	7.36525554	3.41985018	1.30806782
C	19.38399420	1.93145602	-1.59698326
C	20.66535701	1.35605545	-1.79806223
C	19.16799421	3.27906585	-1.86624056
C	21.69332271	2.16855083	-2.31220073
C	20.21118836	4.08301678	-2.34857646
H	18.18758201	3.70019532	-1.69707769
C	21.47096216	3.50924575	-2.58118495
H	22.67503996	1.73316674	-2.47675245
H	22.27279455	4.13345791	-2.96078055
N	15.11525939	-4.38214841	-0.04568519
N	12.16720585	1.29052658	0.61937315
N	18.34539415	1.06624611	-1.16407217
N	13.04842482	-5.97908812	0.83007917
H	12.38876501	-6.61342760	1.26575768
H	13.21639299	-5.17022027	1.41914773
N	20.86461134	0.00602048	-1.55063636
H	21.83373735	-0.29056294	-1.56311396
H	20.38045925	-0.36517308	-0.74010218
N	11.88804855	4.02008940	0.87305146
H	11.74742896	4.99493078	1.11230383
H	12.71829294	3.65016837	1.32377569
C	17.67124647	-8.45400465	-1.35624424
O	17.78610783	-9.66103854	-1.50771536
O	18.66172403	-7.59363187	-1.70208382
H	19.39042132	-8.13418596	-2.06027687
C	7.25968393	0.74888320	1.20680791
O	6.12584283	1.23716855	1.32216546
O	7.48104555	-0.55978715	1.16212171
H	6.61124072	-1.05750675	1.23985874
C	20.02502893	5.51856791	-2.63755278
O	20.88840591	6.26036260	-3.08190606
O	18.77392274	5.96453394	-2.36030827
H	18.75748919	6.91307490	-2.58719549
C	-5.04765182	-1.07179686	1.92715093
C	-5.38135077	0.28398872	1.91298225
C	-4.38558316	1.26634518	1.99129977
C	-3.04933087	0.87862368	2.10976507
C	-2.69919476	-0.47745330	2.11981104
C	-3.70220024	-1.44502694	2.03886847
H	-6.41068344	0.62332780	1.87353185
H	-2.24964718	1.60147512	2.22878957
H	-3.48028756	-2.50496113	2.09535248
C	-6.05683574	-2.18838956	1.87859199
C	-4.84790061	2.69937057	1.98814770
C	-1.23777565	-0.80325695	2.27415870
H	-7.39916188	-0.95370591	0.93746015
H	-3.03309927	3.29532761	1.23842149
H	-1.52736687	-2.54103471	1.23384363
O	-5.77253372	-3.31418238	2.28563520

O	-5.99972640	2.99219594	2.30618874
O	-0.46712700	-0.00975267	2.81341094
C	-8.36470864	-2.77418674	1.18507509
C	-8.17340238	-4.07631460	0.74155508
C	-9.67196160	-2.29071833	1.45251835
C	-9.26859418	-4.93202606	0.54550278
H	-7.16837758	-4.42709335	0.55412107
C	-10.76450100	-3.14977622	1.21809093
C	-10.56790636	-4.44688065	0.77685153
H	-11.77027973	-2.78656089	1.41035551
H	-11.42278813	-5.09572492	0.62182224
C	-4.15143282	5.02578545	1.48076880
C	-5.32950034	5.53107787	0.94640033
C	-3.11266721	5.90268011	1.88827846
C	-5.50981114	6.91488670	0.79612078
H	-6.11074493	4.84539881	0.65014854
C	-3.29545025	7.28819029	1.70407307
C	-4.47187842	7.78624811	1.17136707
H	-2.50324511	7.96793090	2.00535436
H	-4.59640581	8.85713506	1.05448521
C	0.47122062	-2.54130124	1.75680210
C	0.60153788	-3.95419217	1.80870548
C	1.60033075	-1.73646140	1.65000195
C	1.88780675	-4.51569125	1.70501107
C	2.87843423	-2.31096132	1.57965586
H	1.48510521	-0.66285371	1.62306788
C	3.00832304	-3.70862000	1.59307651
H	1.99351644	-5.59664960	1.73537268
H	3.99730396	-4.14944473	1.53104254
N	-7.28110619	-1.87022535	1.35198143
N	-3.91827074	3.62881085	1.60073011
N	-0.84576999	-2.01443241	1.76741473
N	-9.85653730	-0.98888996	1.87536625
H	-10.78109902	-0.77025220	2.22699891
H	-9.12742467	-0.60685684	2.46708673
N	-0.53133920	-4.74991286	1.89217826
H	-0.35016547	-5.73094113	2.07102993
H	-1.26744678	-4.40080491	2.49671340
N	-1.93357646	5.39294441	2.39457337
H	-1.32117931	6.06533940	2.84059990
H	-2.01264487	4.53685378	2.93163215
C	-9.08498804	-6.31880610	0.09111935
O	-10.03674909	-7.09015581	-0.10463392
O	-7.81395921	-6.67299782	-0.09087078
H	-7.71168666	-7.61728832	-0.39913592
C	-6.75224592	7.46833334	0.23615319
O	-6.92809718	8.68545149	0.07248899
O	-7.66676115	6.55310001	-0.08030036
H	-8.49872992	6.94847792	-0.46599446
C	4.08908200	-1.47625909	1.47600757

O	5.22431200	-1.96468225	1.37569289
O	3.86580973	-0.16739668	1.49903395
H	4.73619630	0.33020679	1.42719151
C	-10.09450635	13.13389251	-1.53464278
C	-8.03447388	13.01566563	-0.64546821
C	-9.20267208	11.13791890	-1.04539470
N	-8.06679529	11.68820111	-0.59011279
N	-10.25771827	11.79669388	-1.53280148
N	-9.01781983	13.80780873	-1.10811824
H	-8.34865488	9.34594666	-0.57721138
H	-11.95574318	13.31399719	-2.34410127
H	-6.85655263	14.64075891	-0.22717519
C	-10.19176363	8.91684556	-1.33022264
N	-11.39579528	9.18093872	-1.85921638
H	-11.79122282	10.08693891	-2.08727707
C	-11.25031779	15.21270791	-2.14230339
N	-10.32255323	16.11891194	-1.78818021
H	-9.40985392	15.93831290	-1.38300662
C	-5.79160284	12.99071857	0.32309428
N	-5.60169462	11.66518841	0.47709705
H	-6.22836849	10.89513100	0.24769472
N	-6.89874044	13.62897195	-0.19067773
N	-11.15390201	13.84752909	-2.02817700
N	-9.20685613	9.77896415	-0.97118817
N	-10.07798322	7.59905266	-1.19250112
N	-11.24454833	7.07502997	-1.65225653
N	-12.04530304	8.00175766	-2.05491534
N	-12.30468091	15.85079952	-2.63225554
N	-11.98543484	17.17118180	-2.56316924
N	-10.80721074	17.35315104	-2.06267156
N	-4.71118139	13.62724869	0.75681124
N	-3.86282452	12.65247721	1.17724757
N	-4.37689050	11.47654773	1.01808683
C	-12.18175796	-12.16617263	-1.52525789
C	-13.17447733	-10.25603046	-0.88157965
C	-10.93628633	-10.36471775	-1.05408000
N	-12.01352510	-9.62049605	-0.76076236
N	-10.94318432	-11.64296609	-1.44214942
N	-13.33458038	-11.53580928	-1.26262912
H	-9.84777392	-8.69711138	-0.61459537
H	-11.34758908	-13.93096277	-2.11020448
H	-15.20010217	-10.01273810	-0.67632253
C	-8.49983204	-10.13464699	-1.12836619
N	-8.08674892	-11.35010215	-1.51717596
H	-8.65514911	-12.16330878	-1.72908593
C	-13.35820349	-14.24581948	-2.08912460
N	-14.63293746	-13.86309690	-1.89959164
H	-14.96313655	-12.95044930	-1.60315430
C	-14.34447733	-8.22882349	-0.18105780
N	-13.30351175	-7.39426789	0.01045255

H	-12.30714227	-7.57139473	-0.10858550
N	-14.30609695	-9.54319510	-0.59106661
N	-12.23340783	-13.47620965	-1.92054972
N	-9.76400145	-9.68625113	-0.92059797
N	-7.42821350	-9.36542753	-0.95918916
N	-6.35796304	-10.14855710	-1.25599769
N	-6.72847210	-11.33694553	-1.59162710
N	-13.34653847	-15.51455030	-2.47524600
N	-14.65424398	-15.88701848	-2.51322684
N	-15.43833771	-14.91673564	-2.17335749
N	-15.46695297	-7.57690881	0.09401176
N	-15.07807834	-6.32655452	0.45716177
N	-13.79188356	-6.19944340	0.41331586

## References

1. H.L. Yang, X.W. Sun, Y.M. Zhang, Z.H. Wang, W. Zhu, Y.Q. Fan, T.B. Wei, H. Yao and Q. Lin, *Soft Matter*, 2019, **15**, 9547-9552.
2. A. Kumar, T. Das, R.S. Thakur, Z. Fatima, S. Prasad, N.G. Ansari and D.K. Patel, *ACS omega*, 2022, **7**, 1997-42011.
3. T.B. Wei, Q. Zhao, Z.H. Li, X.Y. Dai, Y.B. Niu, H. Yao, Y.M. Zhang, W.J. Qu and Q. Lin, *Dyes and Pigments*, 2021, **192**, 109436.
4. A. De and R. Mondal, *ACS omega*, 2018, **3**, 6022-6030.